Decoding the effects of synonymous variants

Zishuo Zeng[1*], Ariel A. Aptekmann[1], and Yana Bromberg[1,2*]

1 Department of Biochemistry and Microbiology, Rutgers University, New Brunswick, NJ 08873, USA
2 Department of Genetics, Rutgers University, Piscataway, New Jersey 08854, USA
* Corresponding author: zzeng@bromberglab.org, yana@bromberglab.org
Tel: +1-732-932-9763 Ext. 218; Fax +1-732-932-8965

Abstract

Synonymous single nucleotide variants (sSNVs) are common in the human genome but are often overlooked. However, sSNVs can have significant biological impact and may lead to disease. Existing computational methods for evaluating the effect of sSNVs suffer from the lack of gold-standard training/evaluation data and exhibit over-reliance on sequence conservation signals. We developed synVep (synonymous Variant effect predictor), a machine learning-based method that overcomes both of these limitations. Our training data was a combination of variants reported by gnomAD (observed) and those unreported, but possible in the human genome (generated). We used positive-unlabeled learning to purify the generated variant set of any likely unobservable variants. We then trained two sequential extreme gradient boosting models to identify subsets of the remaining variants putatively enriched and depleted in effect. Our method attained 90% precision/recall on a previously unseen set of variants. Furthermore, although synVep does not explicitly use conservation, its scores correlated with evolutionary distances between orthologs in cross-species variation analysis. synVep was also able to differentiate pathogenic vs. benign variants, as well as splice-site disrupting variants (SDV) vs. non-SDVs. Thus, synVep provides an important improvement in annotation of sSNVs, allowing users to focus on variants that most likely harbor effects.

Availability: synVep webserver for online query: https://services.bromberglab.org/synvep; For local runs Python script (https://bitbucket.org/bromberglab/synvep_local) and prediction database (https://zenodo.org/record/4763256) are also available.

Introduction

The recent increase in accessibility of sequencing has facilitated a rise in precision medicine efforts focused on the interpretation of the effects of individual-specific genome variation (1). Genome-wide association studies (GWAS) have identified multiple variants marking specific phenotypes (2). However, the evaluation of variants in terms of their functional contributions to molecular pathogenicity mechanisms holds promise for both a better understanding of disease and drug discovery/optimization (3). SNVs (single nucleotide variants) are the most common variants in the human genome (4). Three types of SNVs are of particular interest – regulatory (*i.e.* changing the quantity/production of the gene product, *e.g.* transcription or splice site variants), non-synonymous (*i.e.* altering product protein sequence), and synonymous (*i.e.* variants in protein-coding regions that, due to the degeneracy of the genetic code, do not alter the protein sequence). Many computational tools have been developed to evaluate the functional effects of regulatory and non-synonymous variants (5,6). However, while an individual genome carries as many synonymous as non-synonymous SNVs (7), the former are often disregarded as functionally irrelevant. Still, sSNVs can cause disease (8) and affect gene function via multiple mechanisms, including binding of transcription factors (9), splicing (10), mRNA stability (11-13), co-translational folding (14-16), *etc.*, as reviewed in our earlier work (17).

Existing methods for predicting sSNV effects are either (1) sSNV-specific tools, including SilVA (18), reg-SNP-splicing (19), DDIG-SN (20), TraP (21), and IDSV (22), or (2) general-purpose ones, including CADD (23,24), DANN (25), FATHMM-MKL (26), and MutationTaster2 (27). The number of computational sSNV effect predictors is limited in comparison to that of nsSNV effect predictors, as reviewed in (6,17). Partially, this paucity is due to the limited available experimental data evaluating variant effects, which could be used for training or testing of such methods. In fact, all existing predictors, except CADD and DANN, are trained using “pathogenic” variants from databases such as Human Gene Mutation Database (HGMD) (28) and ClinVar (29). Here we note that “pathogenicity” is not equivalent to “functional effect” (30,31) and inferring variant-disease causality is complicated by this inequality. Moreover, the experimental disease variant annotations are often unreliable (17), as it is difficult to distinguish causative variants from simply associated ones. Thus, the pathogenic label is inconsistent across databases, and

possibly over time/database releases. Finally, even these labeled effect variants are few; fewer still, if any, are experimentally labeled neutral polymorphisms. Thus, predictors trained on these variants are likely insufficient to predict the effects of tens of millions of possible sSNVs in human genome.

Here we had inferred, using positive-unlabeled learning (32-34), a subset of human sSNVs that could be used for training a predictor of sSNV molecular effect. We then developed, synVep (Synonymous Variant Effect Predictor), a machine learning-based method for scoring said effect for each possible human sSNV. Notably, synVep does not use conservation as an input feature but is more precise than other predictors (which do use conservation) in discriminating experimentally validated pathogenic sSNVs from randomly sampled observed variants. Its predictions also display the expected trend (35), where the sSNVs that change the human sequence nucleotide to one found in orthologs of evolutionarily-close human relatives, *e.g.* chimp, have lower effect scores than those that change to the nucleotides of further-removed organisms, *e.g.* fly. Furthermore, nucleotides that are not identified in any of the species evaluated here are deemed to have most effect when substituted into the human reference. However, many of the sSNVs that are not observed in the human population, tend to be scored very high (most effect), regardless of their appearance in other species.

In line with our earlier observations (17), we find that the variant frequency in the population is poorly correlated with the effect score. By our definition, common variants have little effect on gene function, but we find that rare variants are about equally likely to be neutral (65% common vs 69% rare neutral variants). To the best of our knowledge, synVep is the first variant-effect predictor that does not rely on conservation and is developed without an experimental or explicitly evolutionarily-estimated gold standard training/development set. Its success also suggests the feasibility of a similar approach for the development of a training set for other variant types, *e.g.* nsSNVs or indels. We expect that synVep sSNV effect predictions will greatly contribute to our understanding of pathogenicity pathways and to the prioritization of synonymous variants in disease.

Materials and Methods

Data Collection. We extracted all 93,437 human protein-coding transcripts from the Ensembl BioMart (36) GRCh37 p.13 assembly (37) and discarded the ones containing unknown nucleotides, lacking a start/stop codon, or having patched (https://grch37.ensembl.org/Homo_sapiens/Info/Annotation) chromosome IDs. We then generated all possible sSNVs for the remaining 72,400 transcripts. We further used ANNOVAR (38) (installed Aug 5, 2019) to extract sSNVs in these transcripts, and their allele-count based frequencies, from the Genome Aggregation Database exome subset (gnomAD exome) (39). An sSNV present in gnomAD was labeled a *singleton* if it was seen in only one individual and otherwise labeled *observed*. *Generated* sSNVs were those in the set of all possible variants in the 72,400 transcripts that were not *singleton* or *observed*. Thus, we collected 4,160,063 *observed*, 3,438,470 *singleton*, and 57,208,450 *generated* sSNVs; https://zenodo.org/record/4763256. Note that these correspond to 1,520,334 *observed*, 1,233,878 *singleton*, and 21,314,668 *generated* sSNVs with unique genomic coordinates and reference/alternative alleles, *i.e.* in one transcript per gene.

To evaluate and compare the performance of our predictor to other predictors, we manually curated a dataset of 42 *curated-effect* sSNVs with known biological effects, including the 33 pathogenic variants from the Buske et al. study (18). We required that all sSNVs in this set were strongly associated with disease and that there was experimental evidence of their molecular effects. These 42 sSNVs (Supplementary Table 1) mapped to 170 transcript-based sSNVs and were excluded from model training throughout this manuscript.

Variant Features. We collected 35 variant and sequence features (Supplementary Table 2), grouped into six categories: codon bias and autocorrelation (10 features), protein structure (3), mRNA stability (8), distance to regulatory factors (4), expression profile (3), and miscellaneous (7).

<u>1. Transcript expression profiles</u>. We downloaded the GTEx (40) "Transcript TPMs" dataset (dbGaP Accession phs000424.v7.p2) and standardized the transcript expression across tissue samples. We then used the average expression of each transcript over all samples from the same tissue as the representative transcript expression for that tissue.

Calculations of some of the codon bias metrics described below require a reference set of coding sequences, which are typically a set of highest expressed transcripts (41). To identify these references, we collected the maximum expression values for all transcripts across the 53 tissues. We then selected the transcripts within the highest 1% expression per tissue. We also used $\log_{10}$ (minimum expression per tissue), $\log_{10}$ (median expression per tissue), and $\log_{10}$ (maximum expression per tissue) for each transcript as features.

2. Codon bias and autocorrelation. A variety of measures and/or their "Δ" form (difference in measure value after mutation vs. value before mutation) are adopted as features to characterize the codon bias of transcripts (see Supplementary Methods for more details), including the Codon Adaptation Index (CAI, Supplementary Methods Eqn. 1) (41), Fraction of Optimal Codons (fracOpt, Supplementary Methods Eqn. 2) (42), Codon Usage Bias (CUB, Supplementary Methods Eqn. 3) (43), Intrinsic Codon Deviation Index (ICDI, Supplementary Methods Eqn. 4) (44), Synonymous Codon Usage Order (SCUO, Supplementary Methods Eqn. 5) (45), and tRNA Adaptation Index (tAI, Supplementary Eqn. 6) (46). The calculation of these values was performed in R (47) and is available as an R package in https://github.com/zengzishuo/codonBiasMetrics.

These measures describe codon bias from different perspectives. CAI, fracOpt, and CUB rely on a reference set of optimal codons, found in highly expressed genes (48). CAI computes the geometric mean of relative usage of a codon compared to the most frequently used codon for the same amino acid (41). fracOpt is the fraction of optimal codons in a sequence of a certain length. CUB weighs the frequency of amino acids in calculating codon bias. ICDI is independent of a reference set of genes (44). SCUO borrows the idea of entropy from Shannon information theory to describe codon usage bias of sequences (45). tAI focuses on translational efficiency by taking tRNA levels into account (46).

We also considered codon autocorrelation – a feature that has not yet been used by any sSNV predictors. In autocorrelated sequences same codons cluster together, whereas they are separated in anticorrelated sequences (*e.g.* XXXYYY is more autocorrelated than XYXYXY, where X and Y are two different codons) (49). Cannarozzi et al. noted the association between codon autocorrelation and translation dynamics and proposed the

tRNA pairing index (TPI) to describe a sequence's codon autocorrelation. Autocorrelated sequences benefit from rapid translation due to the recycling of isoaccepting tRNAs (49). However, we note that the significance of recycling is likely weaker if the interval between two issoaccepting codons is larger – a feature that is not accounted for in TPI. Therefore, we proposed a new measure, Codon Autocorrelation Measure (CAM, Supplementary Eqn. 7), to describe the variant-specific codon autocorrelation impact penalized by the distance between the synonymous codons.

Finally, we also introduced the change of frequency measure (CF, Supplementary Methods Eqn. 8), to describe the amount of impact on codon's frequency in a sequence due to the introduction of the variant.

<u>3. Distance to regulatory and splicing sites</u>. We used as features the distances to the nearest splice sites, transcription factor binding site (TFBS), RNA-binding protein (RBP) motif, and exonic splicing regulator (ESR). Their genomic coordinates were obtained from different sources as described below. We then computed the distance of a variant (in nucleotides) to all regulatory sites and selected the minimum value as the feature distance. We categorized these distances (d) into six categories as feature inputs: d=0, 0<d<=3, 3<d<=5, 5<d<=10, 10<d<=20, and d>20.

Genomic coordinates of regulatory regions were inferred as follows: (1) *Splice sites* were inferred from the "Genomic coding start" and "Genomic coding end" of all human protein-coding transcripts annotated in Ensembl BioMart GRCh37 p.13 assembly. (2) We downloaded the Gene Transcription Regulation Database (GTRD, version 18.06) (50) and identified the genomic coordinates of *TFBS,* using hg38 to hg19 conversion via CrossMap (51) for correspondence with our transcript coordinates. (3) We downloaded the ATtRACT database of RNA binding proteins and AssoCiated moTifs (52) and mapped the human *RPB* motifs to our set of transcript sequences. (4) We also downloaded the supplementary data of Cáceres et al (53) gold standard *ESR* motif set and mapped these to our transcripts.

<u>4. Protein structure.</u> We ran PredictProtein (54), a collection of tools for protein structure predictions, on all of the translated transcript sequences. We were particularly interested in protein secondary structure (PSS), residue solvent accessibility (SS), and disorder (PD)

predictions; in PredictProtein, PROFphd (55) predicts PSS and SS, while Meta-disorder (MD) (56) predicts PD.

5. mRNA stability, structure, and structural changes. We ran RNAfold (57) to predict (with calculation of partition function and base pairing probability matrix) the secondary structure and stability of all transcripts. We extracted the frequency of the structure with minimum free energy (MFE) in the structure ensemble, the free energy of the centroid structure, and its distance to the structure ensemble, as well as the local mRNA structure (strongly paired, strongly up/down -stream paired, weakly paired, weakly up/down -stream paired, or unpaired bases).

We also used RNAsnp (58) to predict the variant-induced local secondary structure changes for all sSNVs. The “mode” and “winsizeFold” parameters should be assigned according to the length in nucleotides (L) of the input sequence. We assigned the parameters as follows: (1) for L <= 200, mod=1 and winsizeFold=100; (2) for 200 < L <= 500, mod=1 and winsizeFold=200; (3) for L > 500, mod=2 and winsizeFold=500. We recorded the local structure dissimilarity, global structural dissimilarity and their statistical significance (p-values).

Model construction

Selecting a classifier. We standardized all continuous features and label-encoded categorical features. We compared two classifiers for differentiating *observed* and *generated* variants: deep neural network (DNN) (59) and XGBoost (60). DNN and XGBoost were implemented in Python (v3.6.4) using Keras (61) (https://keras.io/) and the *xgboost* package (v0.8.2) integrated with sci-kit learn (0.20.3) (62) (https://xgboost.readthedocs.io/en/latest/python/python_api.html), respectively. We split a balanced set (as described below) of *observed* and *generated* sSNVs into training, validation, and testing set in 8:1:1 ratio. Of the two methods, XGBoost was more efficient and achieved higher accuracy in testing and thus was selected as the classifier for future use.

Balancing variant data by transcript. The *generated* set of sSNVs is much larger than the *observed* set, but the number of *observed* sSNVs per transcript varies greatly. Moreover, some classifier input features are transcript-specific. Thus, a predictor may “memorize”

transcripts that have more *observed* sSNVs, and preferentially assign its variants *observed* status, instead of finding variant-specific differences between *observed* and *generated*. To avoid this, we assigned sampling likelihood weights for the *generated* set, *i.e.* the sampling likelihood weight of a *generated* variant is the number of *observed* sSNVs in the corresponding transcript. In all further balancing of data sets, *generated* sSNVs were probabilistically added to the set on the basis of their weights. Thus, the number of *generated* sSNVs on a transcript that were selected for a particular training set was correlated with the number *observed* sSNVs on this transcript.

Positive unlabeled learning (PUL) to identify unobservable sSNVs. PUL is a semi-supervised approach applicable to scenarios where only positive data points are labeled and the rest can be positive or negative (32-34). We employed the modified version of PUL (34) to separate the *generated* sSNVs into *unobservable* and *not-seen* sets. To prevent overfitting, we adopted relatively conservative hyperparameters of XGBoost (100 trees [n_estimor], 5 maximum depth [max_depth], 30% of the features per tree [colsample_bytree], 30% subsamples per tree [subsample]). We left out from PUL a fraction of *observed* as a test set, aiming to reach <5% incorrect predictions for this set at the end of the PUL.

In one epoch of PUL, a classifier was trained to differentiate the *observed* sSNVs from the same number of unlabeled ones (*generated;* selected via transcript-based set balancing as described above). All unlabeled sSNVs, including the ones not used in training, were evaluated with the resulting model and those classified as *observed* (scoring below 0.5) were added to the *not-seen* pool. The PUL process was repeated until convergence (Supplementary Methods). sSNVs scoring >0.5 in prediction from the last PUL model were further excluded from our data set.

Differentiating the observable from not-seen using an intermediate model. We trained a model to differentiate the *observable* sSNVs from the *not-seen* sSNVs (termed intermediate model from here on). We excluded 10% (9,274) of the common sSNVs (MAF > 0.01; *excluded* set) and all *curated-effect* sSNVs (170) from the construction of intermediate model for testing and final model parameter optimization. We split the *observed* sSNVs into subsets of 9: 0.5: 0.5 size ratio for training (3,631,441 variants),

validation and testing (201,746 variants each). We then randomly sampled the *not-seen* variants to match the *observed* validation and test set sizes; this left 47,923,258 *not-seen* sSNVs for training. We then up-sampled the 3.6M *observed* variants in the training set to create a balanced set of 47,923,258 *observed* and *not-seen* variants, each). We tuned the model hyperparameters by optimizing the F1 measure (Eqn. 3) of performance on the validation set and evaluated the resulting model on the test set.

$$Precision = \frac{TP}{TP+FP} \qquad \textbf{(Eqn. 1)}$$

$$Recall = \frac{TP}{TP+FN} \qquad \textbf{(Eqn. 2)}$$

$$F1\ measure = \frac{2 \times Precision \times Recall}{(Precision+Recall)} \qquad \textbf{(Eqn. 3)}$$

where TP, TN, FP, FN are respectively, true positive, *i.e. observed* sSNVs predicted to be *observed*; true negative, *not-seen* sSNVs predicted to be *not-seen*; false positive, *not-seen* sSNVs predicted to be *observed*; false negative, *observed* sSNVs predicted to be *not-seen*.

Final model (synVep) training. We used the intermediate model to score the excluded common and *curated-effect* sSNVs, as well as all *observed* and *not-seen* sSNVs. Here we assumed that common variants should be enriched in no-effect/neutral variation. Based on the scores of excluded sSNVs, we defined *effect* and *no-effect* synVep development sets, where sSNVs (both *observed* and *not-seen*) scoring above the median of the *curated-effect* predictions were deemed *effect*; while sSNVs (both *observed* and *not-seen*) scoring below the median of the excluded common sSNV predictions were labeled *no-effect*. We thus collected 7,385,137 *no-effect* and 32,117,625 *effect* sSNVs.

We split the *no-effect* and *effect* sSNVs into subsets of 9: 0.5: 0.5 size ratio (in the same way as for the intermediate model) for training, validation, and test sets (62,758,222: 735,194: 735,194 variants per set). We sampled equal numbers of *effect* sSNVs to match the *no-effect* sSNVs in validation and test sets. We trained the final model on the training set using the hyperparameters optimized (F1 measure; Eqn. 3) on the validation set. We finally evaluated the model on the test set. Note that none of the *curated-effect*, the *excluded* common sSNVs, or the ClinVar (described below) dataset variants were included in our model training.

Performance comparison with other predictors. To evaluate synVep in comparison with other predictors, we used the 170 (transcript-based*;* 42 genomic coordinate-based) *curated-effect* sSNVs and the 9,274 (transcript-based; 7,957 genomic coordinate-based) *excluded* common sSNVs. Here we again assumed that common variants should be enriched in no-effect/neutral variation.

Other predictors in this comparison included CADD (phred-like scaled scores) (23), DANN (25), FATHMM-MKL (26), DDIG-SN (20), and EIGEN (63). EIGEN scores werere collected using ANNOVAR (38) annotations; for other predictors, the scores were collected with default parameters as described in our earlier work (17). We did not include SilVA (18) or TraP (21) in this comparison because 33 of 42 of the *curated-effect* sSNVs are in their training sets.

Note that synVep scores are produced per variant per transcript, while other predictors use the genomic coordinates, *i.e.* one reference sequence per variant. For the purposes of our comparison, we randomly re-sampled each tool's predictions of the *effect* set (42 variant scores) to produce 170 scores. Furthermore, as the common sSNVs (putatively no-effect) outnumbered the *effect* set, we randomly sampled 170 common variant scores in 100 comparison iterations. For each re-sampling, we performed a one-sided permutation test (null hypothesis: mean of common variant scores is equal to mean of *effect* scores; alternative hypothesis: mean of common variant sores is lower than mean of *effect* scores) and recorded the p-value and the difference of the common and *effect* variant score distribution medians (Δmedians). To assure that all predictor scores fall into the same [0,1] range, we standardized CADD and EIGEN Δmedians to their maximum non-outlier score (20 for CADD and 3 for EIGEN).

We also computed the Spearman correlation across predictor scores and the Fraction of Consensus Binary Predictions (FCBP; *i.e.* the number of binarized predictions agreed upon by all predictors, divided by total number of predictions) (17). An *effect*/*no-effect* scoring threshold for the FCBP computation is required; we used the default value of score=0.5 for DANN, FATHMM-MKL, and DDIG-SN. For CADD, we used score=15 as the threshold recommended by its online documentation (https://cadd.gs.washington.edu/info). As there was no recommended cutoff in the EIGEN

publication (63), we selected the cutoff (score=1.35) at the 75-percentile of EIGEN scores of 1,000 randomly sampled *observed* sSNVs.

ClinVar data analysis. We downloaded all ClinVar (64) submissions from the FTP site (https://ftp.ncbi.nlm.nih.gov/pub/clinvar/) and identified the sSNVs among these. We only considered the sSNVs with the "reviewed by expert panel" *review status*. From these we selected the (1) pathogenic and pathogenic/likely pathogenic variants as the *pathogenic* set and (2) benign and benign/likely benign as the *benign* set. There were 51 *benign* (genomic coordinate-based; 254 transcript-based) and 17 *pathogenic* (genomic coordinate-based; n=68 transcript-based) sSNVs (Supplementary Table 3). We also mapped to these ClinVar sSNVs to the precomputed GERP++ scores (http://mendel.stanford.edu/SidowLab/downloads/gerp/) (65).

Cross-species sequence variation (CSV) analysis. Cross-species variation (CSV) describes the nucleotide difference between the human reference sequence and the ortholog reference sequence of another species. In this study, we selected 20 species to generate CSVs: yeast (*Saccharomyces cerevisiae*), worm (*Caenorhabdiis elegans*), fruitfly (*Drosophila melanogaster*), zebrafish (*Danio rerio*), xenopus (*Xenopus laevis*), anole lizard (*Anolis carolinensis*), chicken (*Gallus gallus*), platypus (*Ornithorhynchus anatinus*), opossum (*Monodelphis domestica*), dog (*Canis familiaris*), pig (*Sus scrofa*), dolphin (*Tursiops truncatus*), mouse (*Mus musculus*), rabbit (*Oryctolagus cuniculus*), tree shrew (*Tupaia belangeri*), tarsier (*Carlito syrichta*), gibbon (*Nomascus leucogenys*), gorilla (*Gorilla gorilla*), bonobo (*Pan paniscus*), and chimpanzee (*Pan troglodytes*).

To represent the evolutionary distance of the CSV species to human, we obtained the value in million years since divergence from the TimeTree database (66). Given a human transcript *T* and its corresponding human gene *G*, we queried Ensembl BioMart for *G*'s orthologs in the 20 species, $\mathbf{G_{orthologs}} = [G_{yeast}, G_{worm}, G_{fruitfly}, \ldots, G_{chimpanzee}]$. We downloaded all coding DNA sequences (CDS) for these orthologs from Ensembl (release-94) (67). For each gene in $G_{orthologs}$, we identified its longest transcript per organism, $\boldsymbol{T_{orthologs}} = [T_{yeast}, T_{worm}, T_{fruitfly}, \ldots, T_{chimpanzee}]$. We then used PRANK (68) to generate a multiple sequence alignment (MSA) for each *T*. PRANK aligns CDSs by first translating them into protein sequences so that gaps tend to be placed between codons, instead of

within codons. For each codon in each human transcript, we could identify if other organisms carried the same codon or another, even if the amino acid remained the same. If the codon was different, the corresponding human sSNV was termed a CSV.

Evaluation of synVep predictions and splicing effects. We downloaded and analyzed a dataset of SNV splicing effects (69) (https://github.com/KosuriLab/MFASS), referenced by genomic coordinates and Ensembl transcript IDs.

Evaluation of synVep predictions according to constraint on coding regions. Constrained regions (70), referenced by genomic coordinates, were downloaded from https://s3.us-east-2.amazonaws.com/ccrs/ccr.html. The constraint of human coding region is measured by percentile (of residuals from a linear regression for distance-to-mutation prediction as computes in (70)), where a high percentile indicates a more constrained the region. We annotated the sparsity of sSNVs, *i.e.* the fraction of *observed* sSNVs among all possible sSNVs in a region of a certain constraint level, and the median synVep prediction of variants in these regions.

Analysis of sSNVs identified in Qatari Genome . We downloaded all VCF files containing variants identified from Qatari Genome project (QTRG) (71) from NCBI Sequence Read Archive (72) (https://trace.ncbi.nlm.nih.gov/Traces/sra/?study=SRP061943). We then parsed these VCF files, extracted the variants, and mapped the sSNVs to our *observed*, *singleton*, *not-seen*, and *unobservable* sets.

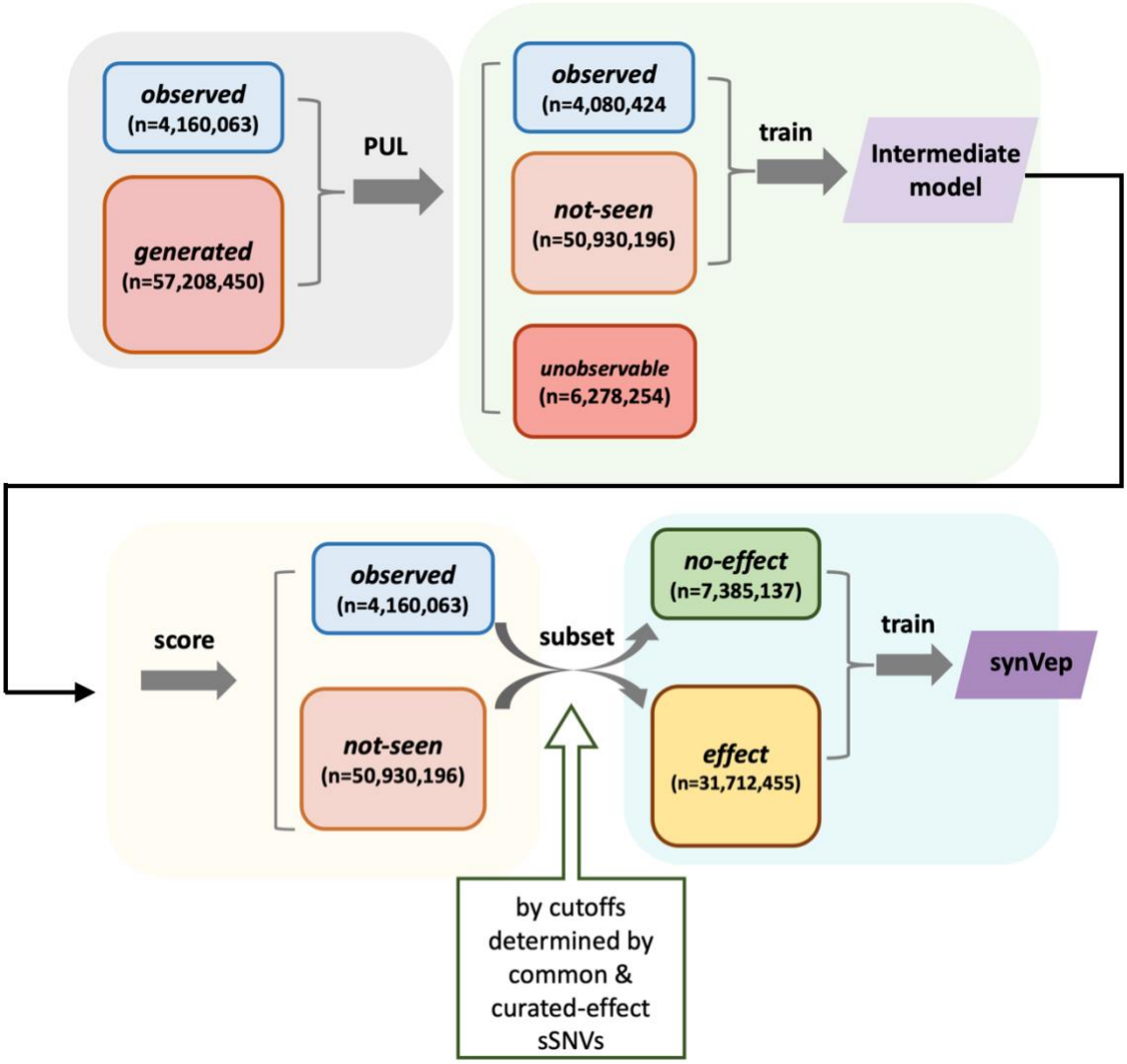

Figure 1. Pipeline of predictor construction. Starting with 4,160,063 *observed* and 57,208,450 generated sSNVs, 63 epochs of positive unlabeled learning (PUL) was conducted to separate the generated set into *not-seen* and *unobservable* set (Supplementary Methods). An intermediate model was trained using the *observed* and *not-seen* sets (*observed* set was up-sampled to equal amount of *not-seen* variants). Intermediate model's predictions for common and pathogenic sSNVs were used as guideline to set cutoffs assigning *no-effect* and *effect* set. The final predictor was trained using the *no-effect* and *effect* sets (*no-effect* set was up-sampled to equal amount of *effect* sets).

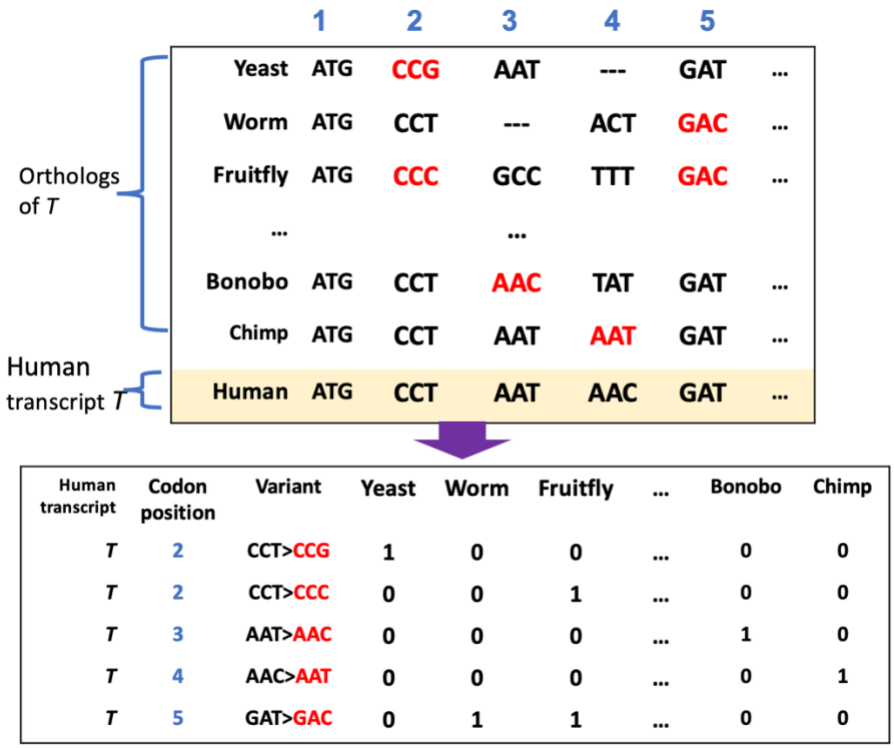

Figure 2. Extraction of cross-species sequence variants (CSV). For each human protein coding transcript *T*, codon-oriented multiple sequence alignment was performed with 20 species' longest coding sequencing of the same ortholog as *T*. The CSV are represented as "codon>codon" format for specific transcript positions and may coincide with human sSNVs.

Results and Discussion

Generated sSNVs may be observable in the future. In the absence of a gold-standard experimentally validated data set describing sSNV functional effects, we sought an alternative for the development of our method. We had previously proposed to use sSNVs that have been *observed* in major sequencing projects *vs.* all other possible human genome sSNVs (the *generated* set) for method evaluation (17). We collected (Methods) 72,400 human transcripts with 4,160,063 (n=1,520,334 genomic coordinate-based) *observed* sSNVs and 3,438,470 (n=1,233,878 genomic coordinate-based) *singletons,* observed in only one individual, from the exome sequencing data of the Genome Aggregation Database (gnomAD exome) (39). We then created a *generated* set of 57,208,450 (n=21,314,668 genomic coordinate-based) all possible sSNVs in these transcripts that were not found in gnomAD data. Note that only ~12% of all sSNVs in our set were ever observed. We annotated these sSNVs with 35 transcript- and variant-specific features, including codon bias, codon autocorrelation, transcript stability,

expression level, distance to regulatory sites, predicted protein secondary structures, *etc.* (Methods and Supplementary Table 2). Notably, we did not include any conservation-related features.

While the *observed* sSNVs are not necessarily functionally neutral, they are at least compatible with life. The *generated* sSNVs, on the other hand, are likely split of two subtypes: the *not-seen* sSNVs, which may or may not become *observed* with more sequencing, and the *unobservable* ones, which cannot be observed given the contemporary variant-discovery capability. Note that the *unobservable* character of sSNVs may be due to a broad range of technical and biological reasons such as sequencing (73,74), molecular functional constraints (75), and analytical biases or extreme deleteriousness resulting in early embryonic incompatibility with life (76,77). We also note that in our modelling, the *unobservable* set may simply be poorly described by our selection of variant features, which capture the *observed* and *not-seen* sSNVs.

We used *observed* sSNVs as positives in positive-unlabeled learning (PUL) (32-34) to differentiate the *not-seen* sSNVs (similar to *observed*) from *unobservable* ones in the *generated* (unlabeled) set. At convergence (epoch 63, Methods; Supplementary Fig. 1), PUL partitioned all *generated* sSNVs into *unobservable* (n=6,278,254 transcript-based and 2,764,229 genomic coordinate-based; 11%) and *not-seen* (n=50,930,196 transcript-based and 19,730,623 genomic coordinate-based; 89%). Additionally, 8% (n=266,192) of *singletons* were deemed *unobservable* by the PUL model, as were 2% of the *observed* sSNVs (n=79,639). The latter result highlights the possible insufficiency of our variant descriptors for capturing the complete observable variant diversity, while the former may also indicate sequencing errors. The difference in percentages of variants misidentified by the model (11% of *generated* vs 2% of *observed*), however, suggests that deleteriousness of variants also plays a role in defining *unobservable* variants.

<u>*Observed and not-seen variant sets contain both no-effect and effect sSNVs*</u>. We trained the *intermediate* model (Methods) to recognize *observed* vs. *not-seen* sSNVs. The model accurately (F1=0.71; Eqn. 3) recognized the two classes in a previously unseen variant test set (Supplementary Fig. 2). The model also predicted 9% (9,282,542) of the *not-seen*

sSNVs to be *observed* (scoring < 0.5), implying that these may be sequenced in the future.

While observed sSNVs are likely depleted in large functional effects, they are not all functionally neutral; for example, pathogenic sSNVs are, in fact, observed. Similarly, not all *not-seen* sSNVs have a functional effect; rather, they may be observable in the future. To build a model for evaluating the effects of sSNVs, we leveraged the intermediate model's predictions on common variants *excluded* from training and the experimentally validated *effect* sSNVs (*curated-effect*; Methods; 170 transcript-based sSNVs). While these *curated-effect* sSNVs are, in fact, observed, their prediction scores were higher than those of the *excluded* common set (Supplementary Fig. 2, Mann-Whitney U test p-value<2.2e-16). This observation is likely due to the fact that the *not-seen* set is enriched. while the common variant set is depleted, in large effect sSNVs. We assume this for common variants because large-effect deleterious variants would not become common and large-effect advantageous variants would tend to become wild-type.

We excluded 10% (7,957) of the common sSNVs from training of the intermediate model for selecting the cutoff of *effect/no-effect* variants as next described. For training of the final model, we selected as *no-effect* those sSNVs (both *observed* and *not-seen*) scoring below the intermediate model prediction median (0.38) of the excluded common sSNVs; variants scoring above the intermediate model median of the *curated-effect* sSNVs (score = 0.63) were labeled *effect* (Supplementary Fig. 2). We thus obtained 7,385,137 (2,580,540 *observed* and 4,804,597 not-seen) *no-effect* and 32,117,625 (405,170 *observed* and 31,712,455 *not-seen*) *effect* sSNVs. We trained the final model (synVep) to differentiate the *no-effect* and *effect* sSNVs (in balanced class training), using a 9: 0.5: 0.5 split of data for training, validation, and testing purposes (Methods). synVep was accurate (F1 measure=0.90; binary score cutoff=0.5) in evaluating the previously unseen test set (369,257 *no-effect* and 369,257 *effect*). For the same set, the F1 measures of the CADD, DANN, DDIG-SN, FATHMM-MKL, and EIGEN performance were 0.03, 0.48, 0.03, 0.46, and 0.46, respectively.

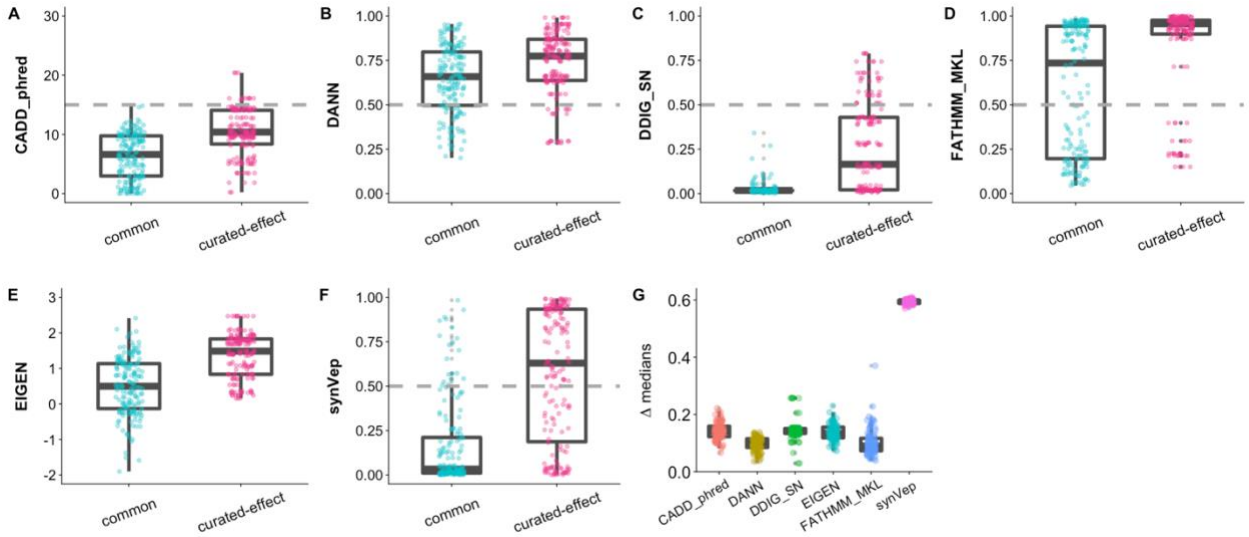

Figure 3. Predictor performance on common *vs. curated-effect* sSNVs. Panels **A-F** show the differential predictions on sets of *curated-effect* (n=170) and common sSNVs (randomly selected n=170) for CADD (phred-like scaled scores), DANN, DDIG-SN, FATHMM-MKL, EIGEN, and synVep, respectively. Gray line indicates scoring cutoff suggested by tool authors. Neither the common set nor the *curated-effect* set were included in synVep training. In panel **(G)**, this comparison was repeated 100 times to compute the Δ medians (i.e., $\text{median}_{\text{curated-effect}} - \text{median}_{\text{common}}$). Permutation tests show that all of the predictors give significantly different scores between the two sets in every iteration, except for DANN where two of 100 comparisons were not significant (p-value>0.05 after Bonferroni correction).

<u>*synVep outperforms other predictors in identifying effect sSNVs.*</u> In order to evaluate the performance of our method, we needed a gold standard set of designated effect and no effect variants. However, since there are no experimentally validated "neutral" sSNVs, we used the common sSNVs never seen in training as neutrals (*no effect*), *i.e.* as described above we assumed that the majority of common sSNVs have little effect. On the level of molecular function, the *effect* of a variant is not directional (neither advantageous nor deleterious). On the level of individual fitness (evolutionary), however, variants could be advantageous, neutral, or deleterious. Note that evolutionarily *effect* variants must have a molecular *effect*, but not vice versa. The neutral theory of molecular evolution, as well as some experimental work, suggest that advantageous mutations are rare, and most effect mutations are deleterious (78,79). Variants with large deleterious effects on evolutionary fitness would have been purified out and will not be seen in the population. Neutral or weak *effect* mutations could, depending on the population size, become

common or even fixed due to genetic drift (78). Thus, in the absence of experimentally neutral variants, common variation may be considered a reference point for neutral or weak *effect* variants.

We used the set of *curated-effect* sSNVs as the *effect* group. Note that these sSNVs, as well as any other sSNVs in their corresponding transcripts, were never used in our model training. Since the test set of no effect common variants (9,274 sSNVs) greatly outnumbered the *curated-effect* set (170), we randomly sampled 170 sSNVs from the common set 100 times (Methods). Predictor scores were significantly different (p-value < 0.05 after Bonferroni correction for multiple hypothesis testing; Fig. 3A-E; Methods) between variant groups in all 100 rounds; the sole exception was DANN, where in 11 of 100 rounds the differences were not-significant (p-value > 0.05). Notably, the difference in median scores between the *effect* and *no-effect* variants was at least two-fold greater for synVep than for other methods (Fig. 3F; CADD and EIGEN scores normalized to 0-1 scale). Furthermore, while all predictors identified most *curated-effect* sSNVs as having more *effect* than common sSNVs, most failed to differentiate the two at the default method binary prediction threshold. synVep's predictions fulfilled this criterion, while other predictors either placed both sets of variants below (CADD, DDIG-SN) or above the default threshold (DANN, FATHMM-MKL).

We further examined the correlation of the predicted scores (Fig. 4A) and the Fraction of Consensus Binary Prediction (17) (FCBP; Fig. 4B) on all 4,160,063 *observed* sSNVs for all predictors (synVep, CADD, DANN, FATHMM-MKL, DDIG-SN, and EIGEN). synVep's scores were poorly correlated with other predictor scores (Pearson correlation ranging from -0.1 [DANN] to 0.21 [FATHMM-MKL]), while binary classification was more similar (FCBP ranging from 0.37 [DANN] to 0.69 [CADD and DDIG-SN]).

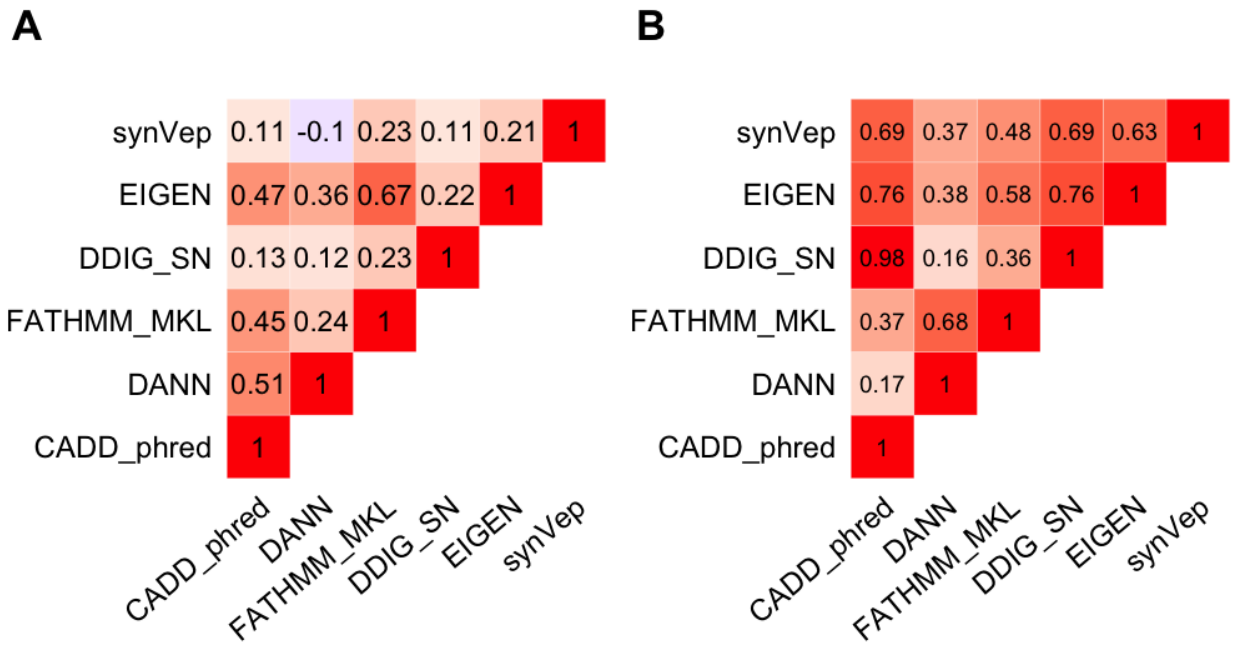

Figure 4. Comapring predictions made by synVep and other tools. Panel **(A)** Spearman correlation and **(B)** Fraction of Consensus Binary Prediction (FCBP) highlight similarity and lack thereof among the predictors for all *observed* sSNVs (n=4,160,063).

<u>*Singletons are more likely than observed to be effect.*</u> *Singletons* were not included in our training because it is difficult to estimate how many of them are artifacts due to the 0.1-0.6% error rates of next-generation sequencing (80). If the *singletons* are not artifacts, then they are likely to be individual or ultrarare variants. These are more likely to be *effect* than higher frequency variants (81,82). An excess burden of ultrarare variants (although not necessarily synonymous) is also often seen in diseases, such as schizophrenia (83-85), Parkinson disease (86), and bipolar disorder (87). In line with these expectations, we found that *singletons* were, on average, scored higher than *observed* sSNVs (Supplementary Fig. 3), suggesting that *singletons* are more likely to be *effect* than the *observed*.

<u>*Variant effect predictors differentiate benign and pathogenic variants*.</u> Among the predictors considered in this work, only two (FATHMM-MKL and DDIG-SN) are explicitly predictors of variant pathogenicity. To investigate whether predictors of variant *effect* (not pathogenicity) can identify pathogenic sSNVs, we obtained from ClinVar (reviewed by

expert panel) 17 *pathogenic* (genomic coordinate-based, 68 transcript-based) sSNVs and 51 *benign* sSNVs (genomic coordinate-based, 254 transcript-based). Of these, one benign and one pathogenic variant (genomic coordinate-based, 13 transcript-based) were deemed unobservable by our model and were removed from consideration. Note that, for fairness of evaluation, these sSNVs were excluded from training synVep.

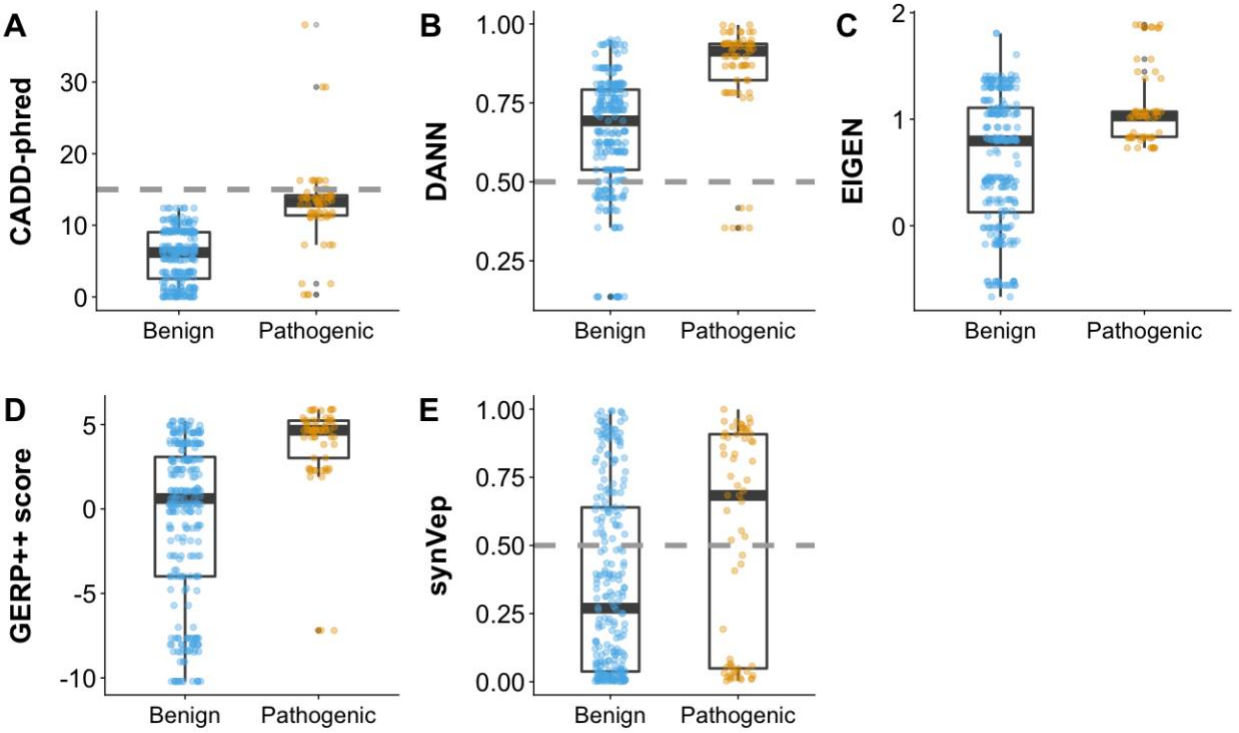

Figure 5. Evaluating variant effect predictors using ClinVar data. *Benign* are variants labeled "Benign" and "Benign/Likely benign" in ClinVar, with "Review by expert panel" as review status. *Pathogenic* are those labeled "Pathogenic" and "Pathogenic /Likely Pathogenic" in ClinVar, with "Review by expert panel" as review status or with "research" method and at least one publication experimentally validating the *effect*. Panel A-E show the predictions from for CADD (phred-like scaled scores), DANN, EIGEN, GERP++ score, and synVep, respectively. Grey dashed lines show the method author-recommended cutoffs, where available.

All variant-effect predictors, including synVep, assigned higher scores to *pathogenic* than *benign* variants (Fig. 5A-C and E, all statistically significant, one-sided permutation test p-value = 0). Importantly, note that all variant-effect predictors except synVep use GERP++ (65) as a feature. GERP++ identifies constrained elements in multiple sequence alignments and is thus a feature reflective of conservation. Highly conserved genomic

positions often have experienced extensive purifying selection (88). Therefore, conservation is understandably a commonly used feature for disease variant prioritization (89). The area under the precision-recall curve (PR AUC, Eqn. 1,2) measures for CADD, DANN, EIGEN, and synVep were 0.60, 0.62, 0.70, and 0.73, respectively, suggesting that synVep provides the best discriminative power on this rigorous expert-reviewed disease variants dataset. Note that GERP++ attained 0.62 PR AUC, meaning that the performance of the specialized predictors did not substantially improve or was worse than that of one of their features, i.e. GERP++. Also note that at the default/recommended cutoff, only synVep placed the majority of *benign* vs. *pathogenic* variants on opposite sides of the cutoff (precision=0.32, recall=0.60). Here, the method's low precision indicates that many of ClinVar labeled "benign" variants likely carry functional effects, which may not manifest as disease. Moreover, in the scenario of disease variant prioritization synVep offers discriminative power independent of conservation, so it may be used in combination with a conservation score or other predictors.

One major challenge in disease variant prioritization is that for complex diseases, causality can rarely be explained by a single variant (90). The utility of variant pathogenicity score is thus questionable: does a high score suggest a high likelihood of an individual developing a disease or a high likelihood of this variant contributing to a disease? Also, would an individual with many predicted-pathogenic variants carry many diseases or be very certain to carry at least one disease? One potential way to bypass this puzzle is to establish the variant-disease relationship with the collective *effect* from the whole variome, instead of a single or a few variants. One way to use the effect information could be to optimize the polygenic risk scoring methods (91,92) to only focus on effect variants. However, this approach would be limited by the location of most SNPs in non-coding regions. Attempts to unite variant effects across the coding region of the genome (e.g. (93), (94)) measure every gene product's change by aggregating all variants per gene (as a burden or as function changes) to predict disease predisposition. As a future application, synVep predictions (as well as other variant effect) may be plugged in these pipelines to explore the contribution of sSNVs to complex diseases.

synVep highlights correlation between conservation and effect. We annotated all sSNVs as CSVs (cross-species variation) or not (Fig. 2; Methods). CSVs are codon differences

between the human reference sequence and another species' ortholog. For example, if the proline-coding codon in a human transcript *T* is CCC, while the aligned proline codon on *T*'s chimp ortholog is CCT, then the human sSNV CCC->CCT is considered a chimp-CSV. We thus annotated 15,618,155 unique (only exists in one species) and 35,102,565 non-unique (overlapping across species) CSVs (Supplementary Fig. 4). Since less than 10% (7,026 of 72,400) of the human transcripts can be mapped to orthologs in all 20 species, we analyzed separately the CSVs in (1) *all transcripts* (n=32,264,860) and (2) only the transcripts that have orthologs in all 20 species (n=3,321,574) and that are likely ancient (*ancient genes*) (95) .

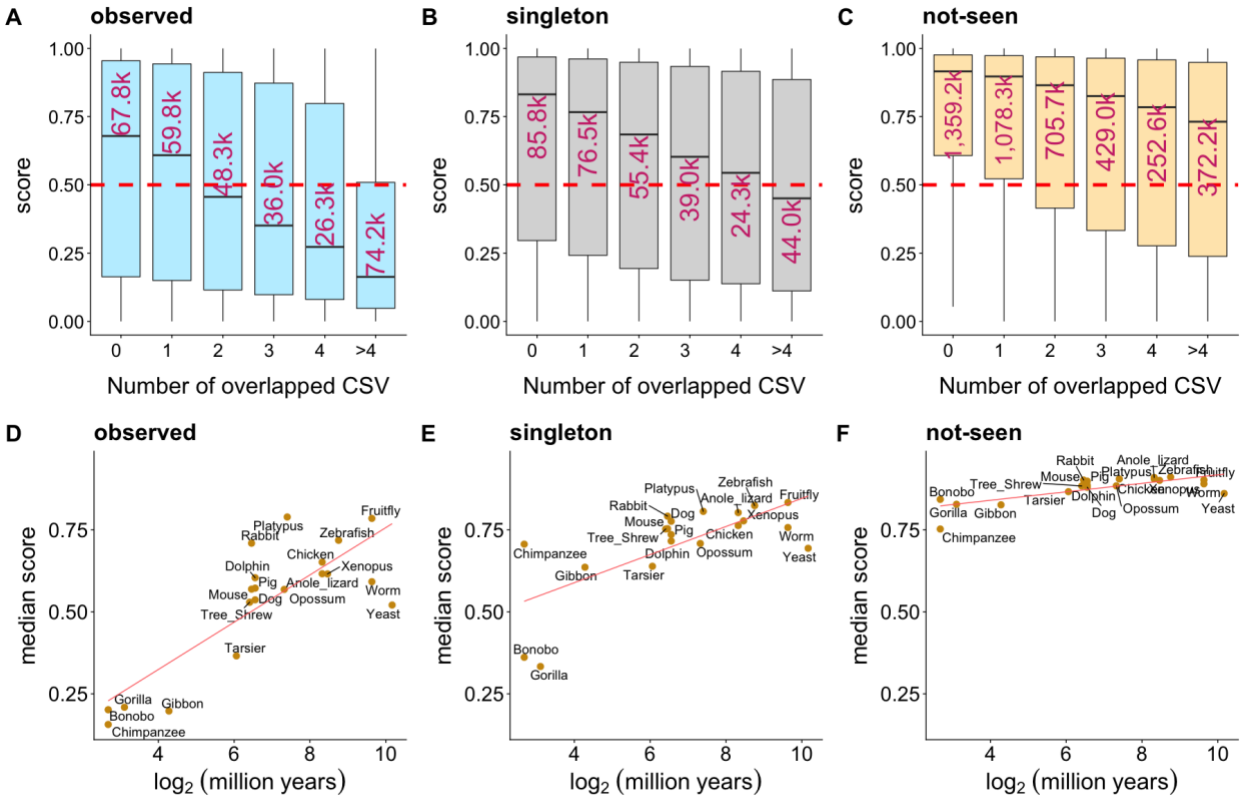

Figure 6. Variant effect prediction from the perspective of cross-species variation (CSV). Panels **A-C** show synVep-predicted scores for variants grouped by the number of species carrying the mutant nucleotide; separately for *observed*, *singletons*, and *not-seen* sets. The red dashed line is synVep's default cutoff for *effect* and *no-effect*. The number in each box indicates the number of variants of that group (in thousands). Panels **D-F** show the median score (y-axis) across species at $\log_2$ million years since divergence from common ancestor with human (x-axis) and linear regression trendline (red line) between the two. The Spearman correlations between median synVep score and log2(million years) for panel D-F are 0.68, 0.64, and 0.66, respectively.

The distribution of synVep prediction scores for CSVs in the *ancient genes* and for those in *all transcripts* were similar (Δmean=0.05, Mann-Whitney U test p-value<2.2e-16), suggesting that synVep*'s* evaluation of variants does not discriminate by gene age. For *all transcripts*, *observed* sSNVs had more CSVs (67%, n=2,823,142) than did the *not-seen* variants (53%, n=26,976,016; Supplementary Fig. 5). CSVs overall were predicted less likely to be *effect* than non-CSV for both *ancient* and *all transcripts* (Fig. 6 A-C; Supplementary Fig. 6 A-C). While this is in line with the scoring trends of the observed and not-seen variants overall, it also mirrors earlier findings of few CSV nsSNVs corresponding to a known human disease (96-99). synVep scores also trended lower for CSVs whose substituting nucleotide was found in more species, for both *ancient* (Fig. 6 A-C) and *all transcripts* (Supplementary Fig. 6 A-C). Since the number of CSV species is somewhat indicative of codon conservation, this trend suggests that, although synVep was trained without using conservation descriptors, its predictions still identify conserved codons that are often functionally relevant (100).

To further elucidate the effect of sequence conservation across species, we calculated codon mutation fraction (CMF, Supplementary Eqn. 9) to describe how common a human's alternative codon is, compared to the reference codon, among the 20 species included for CSV analysis. For example, if in a multiple sequence alignment of the 20 species orthologs, the human CCC codon is aligned to 10 CCC, 5 CCT, and 5 other codons, then the CMF of the corresponding synonymous variant, CCC>CCT, is 5/15=0.33. We observed that predicted scores generally decrease with higher CMF (supplementary Figure 7 A-C), indicating that sSNVs with alternative codons commonly present as reference codons among other species have less *effect*.

We additionally investigated the relationship between the evolutionary distance of CSV species from human and the *effects* of the corresponding sSNVs. Since one sSNV can correspond to multiple species CSVs, we only considered CSVs that are uniquely found in one species for this evaluation. The medians of synVep scores of these species-exclusive CSVs in both *ancient genes* (Fig. 6 D-F) and *all transcripts* (Supplementary Fig. 6 D-F) correlated with the evolutionary distance of the corresponding species to human. However, for ancient genes, the median scores of *observed* variants unique to further related (i.e. beyond Tarsier) species were in the *effect* range (synVep>0.5). Arguably, this

means that human sSNVs that introduce nucleotides likely present in recent ancestors tend to be *no-effect*, while similarity to further removed relatives carries no such benefit (Fig. 6 D). These findings agree with our recent work on nsSNV CSV analysis (35). We note that species relationship had much less impact on binary *effect* classification for singleton variants and none for not-seen variants (Fig. 6E-F). The same observations could not be made for the *all transcript* set of variants, where *observed* and *singleton* CSVs were predicted to be *no-effect* for a large portion of species (Supplementary Fig. 6D-F). This observation suggests that ancient genes are functionally crucial and have been sufficiently optimized over time to only permit minor levels of variation without impact on functionality.

synVep differentiates splice-disrupting variants. Cheung et al. (69) measured the splice-disrupting effects of genomic variants (3,297 transcript-specific sSNVs) and defined a group of large-effect splice-disrupting variants (140 SDV sSNVs). As expected, synVep scores of SDVs were on average higher than those of non-SDVs (Fig. 7 A-C). Curiously, 140 SDVs comprised only six *observed* (4.6%) and 18 *singletons* (13.7%) variants; nine were deemed *unobservable* (6.4%) and 107 were *not-seen* (76.4%). The fact that most of SDVs are *not-seen* reinforces our assumption that *not-seen* sSNVs are enriched for large-effect deleterious sSNVs that may have been purified.

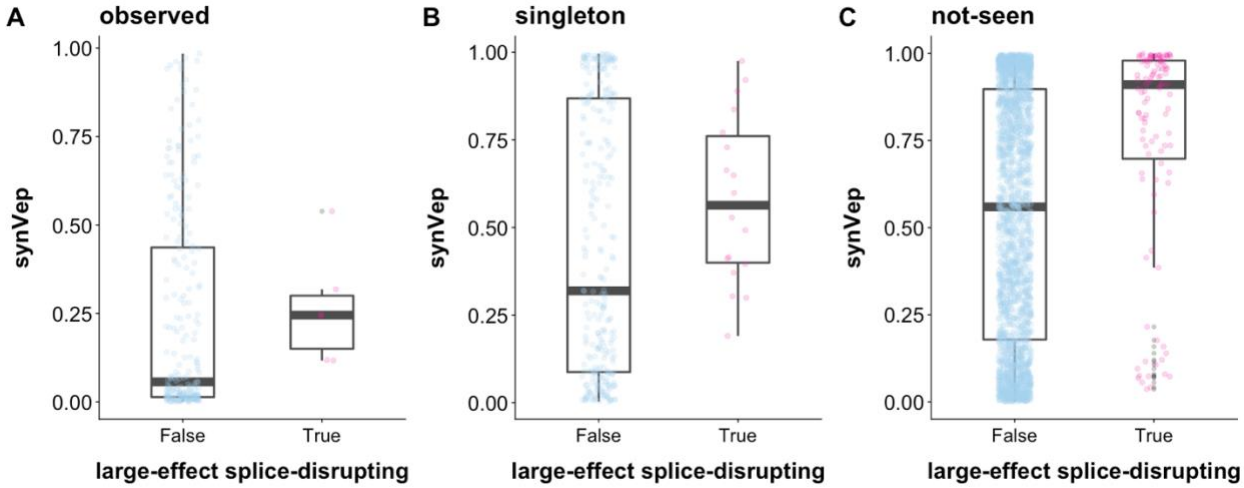

Figure 7. synVep predictions for large-effect splice-disrupting variants (SDVs) and non-SDVs. SynVep predictions are higher scoring for a set of experimentally determined SDV than non-SDV variants across *observed*, *singleton*, and *not-seen* data sets. Note that non-SDVs may

still carry other functional effects. The mispredicted neutral SDVs highlight the limitations of our training data, which is limited in differentiating between effect and no-effect observed variants; although two of the five observed SDVs are correctly annotated as effect.

Splicing disruption is a well-known and well-studied mechanism of sSNV *effect* (101). In fact, most of the experimental validations of our *curated-effect* and ClinVar *pathogenic* variants refer to elucidating splicing effects (Supplementary Table 1 and 3). Moreover, many cancer driver mutations are found to be splice-disrupting synonymous variants (102). Aside from splicing, experimental validation of variant *effect* is rare, arguably due to technical challenges (103). Perhaps, since the experimental evidence for splicing disruption is more abundant than non-splicing effects', the former is considered a major factor in clinical consideration for sSNVs. For example, according to the guidelines from American College of Medical Genetics and Genomics (104), an sSNV is clinically benign if it is not in a conserved position and is predicted to be non-impacting to a splice site (e.g. via GeneSplicer (105), NNsplice (106)). Thus, synVep's ability to identify *effect* and score sSNVs regardless of their splice effects or conservation makes it an ideal tool for prioritization of all possible variants, regardless of their mechanism or evolutionary evidence of *effect*.

sSNV effects are limited by genomic constraints. Havrilla *et al*. developed the concept of "coding constrained regions" (CCR) to describe the regional scarcity of protein-changing (missense or loss-of-function) variants in the human genome (70). Here, a region with fewer of these variants observed in the human population has a higher CCR percentile score. For our set of variants, the fraction of *observed* (number of *observed* sSNVs divided by all possible sSNVs in this region) negatively correlated (Pearson ρ=-0.61) with CCR percentile (Fig. 8 A); *i.e.* higher constrain indicates fewer sSNVs. Furthermore, synVep predictions positively correlated with CCR percentiles for *observed* (ρ=0.58, Fig. 8 B), *i.e.* lower CCR percentile (less constrained regions) indicated lower (*no-effect*) synVep scores.

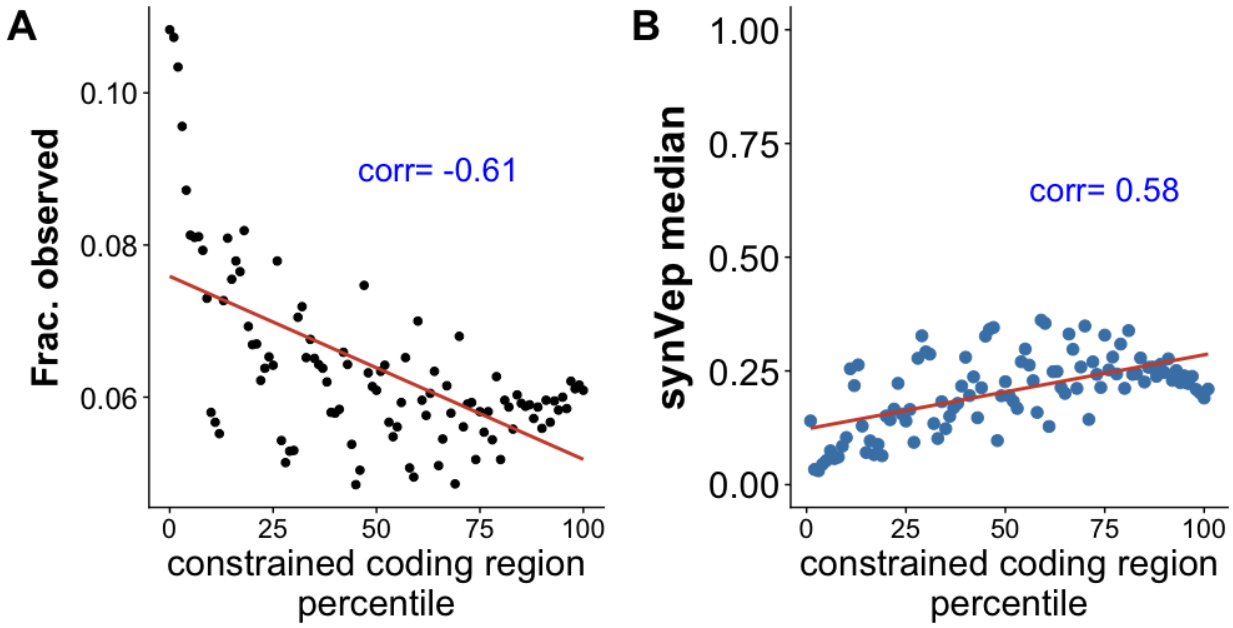

Figure 8. sSNV effect measured by region constraint. Coding constrained regions (CCR) describe the regional scarcity of nsSNVs; higher percentile regions represent have fewer observed nsSNVs. *Observed* sSNVs are relatively scarce in constrained regions **(A)**, while their median synVep scores are higher **(B)**. Pearson correlation are indicated in blue.

The negative correlation between the fraction of sSNVs and CCR indicates a positive correlation between synonymous mutation rate and missense or loss-of-function mutation rate. This observation is in line with earlier studies (107,108), but raises a question of the utility of Ka/Ks ratio (nonsynonymous divided by synonymous mutation rate), which is widely used to measure the strength of evolutionary selection at certain genomic sites (109). The application of the Ka/Ks ratio is based on the assumption that synonymous mutations are neutral and thus Ks can serve as a baseline for Ka. However, it has been demonstrated that a high Ka/Ks can also result from a low Ks due to strong negative selection at the synonymous sites (10,11,110-112). Efforts have been made to improve the utility of Ka/Ks by incorporating codon preference (113-115), but the question remains: how often is the selection at synonymous sites sufficiently underestimated so that Ka/Ks is no longer accurate? Lawrie et al. found that 22% of the fourfold synonymous sites (where the amino acid can be encoded by four codons) in the fruitfly genome are under strong selection (116). Lu and Wu estimated that 90% synonymous mutations in human and chimp are deleterious (117). Hellmann et al. estimated that 39% mutations at

the human-chimp-diverged non-CpG fourfold synonymous sites have been purified (118). Zhou et al. showed that 9% of all yeast genes and 5% all worm genes undergo purifying selection on synonymous sites (115). In turn, our results show that about 67% of all possible human sSNVs (excluding *unobservable*) are *effect* (synVep score>0.5), but we cannot estimate the strength of selection at these sites. Taken together, these observations suggest that Ka/Ks measures of genomic site constraints may be underpowered.

synVep sheds light on future variant discovery and interpretation. Whenever a human genome variant is sequenced, it will automatically be reassigned a class in our collection. Thus, a newly sequenced variant will first become a *singleton* and may, eventually, be a member of the *observed* group. An enrichment in *observed* variants will likely come from large-scale sequencing. Here, it is important to remember that although only 16% of global population are of European descent (119), 45% of the subjects whose exomes are recorded in the gnomAD exomes database (120) are; i.e. there is a significant underrepresentation of sSNVs from other ethnicities. When more diverse genomes are sequenced, will there be a significant addition to the *observed* set (i.e. significant reduction of the *not-seen* set)?

To answer this question, we obtained all variants from the Qatar Genome (QTRG) project (71) and mapped them to our set of sSNVs. QTRG comprises 1,376 individuals and may serve as a representative pool of genomic variants in Middle East and north Africa (MENA) area (71); thus, this set is complimentary to gnomAD. We identified 526,616 transcript-based sSNVs (n=192,246 genomic coordinate-based) from QTRG sequencing. Importantly, only 0.6% of the Qatari sSNVs mapped to our *unobservable* set – a fraction that is lower than the misprediction rate (5%) that we allowed during PUL. Moreover, two thirds of these variants were singletons in QTRG. This observation suggests that our unobservable variants are indeed unlikely to be ever observed in future sequenced human populations. The majority of QTRG sSNVs (81.9%) mapped to our *observed* set; 4.6% and 12.8% were *singleton* and *not-seen*, respectively, in our set (Fig. 9 A). Interestingly, 63.5% and 64.6% QTRG sSNVs mapping to our *singleton* and *not-seen* sets, respectively, were singletons in the Qatari cohort.

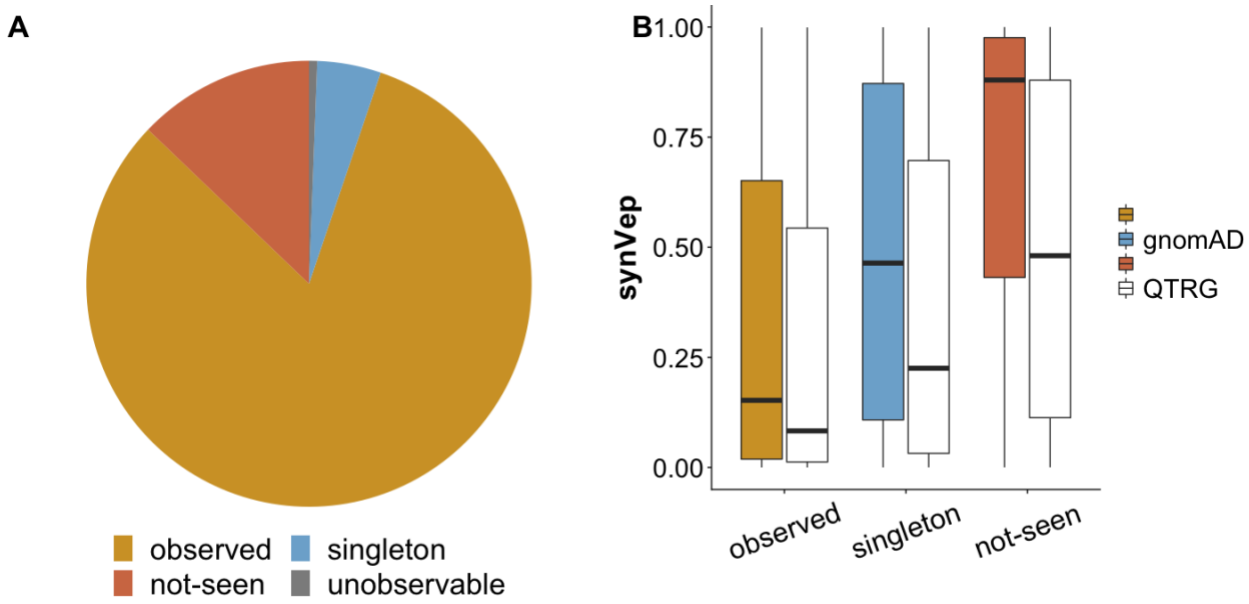

Figure 9. Distributions of the Qatar Genome sSNVs. In both panels, our gnomAD-based *observed* (orange), *singleton* (blue) and *not-seen* (dark orange) sets are highlighted. **(A)** represents the fraction of the QTRG sSNVs mapped our *observed*, *singleton*, *not-seen*, and *unobservable* (gray) sets. **(B)** synVep scores for our (gnomAD-based) variant sets, as well as the scores for QTRG sSNVs (white) mapping to the corresponding gnomAD-classes. Importantly, the synVep scores of QTRG variants that were previously classified as singletons or not-seen score much lower than other variants in the corresponding groups.

How many of the previously *not-seen* sSNVs are *effect*? New sSNVs are likely to come from clinical sequencing and could thus could often be deemed disease-associated. We expect, however, that these variants will carry little or no *effect*. In other words, currently *not-seen no-effect* observable sSNVs (n=14,259,180 transcript-based and n=5,975,076 genomic coordinate-based) are more likely to be discovered in the future than an *effect* ones – even if a sample is taken from a sick individual. Recall our assumption that the *not-seen* set is composed of those sSNVs that carry a large effect and have been purified, as well as those that are putatively neutral and will be seen in the future if more sequencing is performed. The synVep scores of the QTRG sSNVs mapping to our *not-seen* set were, on average, much lower than those of the entire *not-seen* set (Fig. 9 B, average synVep score 0.49 vs. 0.70, Mann-Whitney U test p-value<2.2e-16). This result confirms our assumption, as these newly identified sSNVs are actually observable (not

purified) and thus they are generally less likely to have large effect (and thus lower synVep scores). It may also be that the newly identified predicted *effect* variants (from QTRG, and other sequencing efforts in the future) are the ethnicity-differentiating, i.e. not necessarily affecting overall fitness, but contributing to individual differences (as in e.g. (121)).

Conclusion

We developed synVep—a machine learning-based model for evaluating the *effect* of human sSNVs. Our model does not use disease/deleteriousness-labeled training data or rely on conservation. Instead, we used the signals derived from *observed* (and corresponding *generated*) sSNVs from large sequencing projects. Our model successfully distinguishes sSNVs with experimentally validated *effect*, e.g. splice-site disrupters, as well as pathogenic sSNVs. Moreover, our model's predictions of cross-species variants (CSVs) correlate with the evolutionary distance between human and CSV-species. While further experimental validations of *effect* prediction are necessary, synVep's evaluation on sSNV *effect* will greatly contribute to our understanding of biological molecular pathways in general, and of pathogenicity pathways in particular.

Author contributions

ZZ and YB designed the study, evaluated the results, and wrote the manuscript; ZZ conducted the study; ZZ and AA built the webserver.

Acknowledgements

We thank our current and former lab members, Dr. Yannick Mahlich, Dr. Chengsheng Zhu, Dr. Maximillian Miller, and Dr. Yanran Wang (all Rutgers), for all discussions and constructive suggestions. We also thank Kyle Flannery (Rutgers) for the idea of testing our predictions with Qatari Genome variant data. We are also grateful to the Rutgers Office of Advanced Research Computing (OARC) for making high-performance compute resources available to this project,

Thomas Pawlowski (Rutgers Office of Information Technology) for setting up the host of synVep webserver, and to the Ensembl team for their help and feedback. Last but not least, we want to thank all researchers and human subjects who made the data and tools used in this study available.

Grant support

ZZ and YB were supported by the NIH/NIGMS grant R01 [GM115486]; AA is supported by the Astrobiology Institute grant [80NSSC18M0093]; YB was also supported by NIH grant R01 [MH115958].

Conflicts of interest

None declared.

1. Ashley, E.A. (2016) Towards precision medicine. *Nature Reviews Genetics*, **17**, 507.
2. Visscher, P.M., Wray, N.R., Zhang, Q., Sklar, P., McCarthy, M.I., Brown, M.A. and Yang, J. (2017) 10 years of GWAS discovery: biology, function, and translation. *The American Journal of Human Genetics*, **101**, 5-22.
3. Pan, B., Kusko, R., Xiao, W., Zheng, Y., Liu, Z., Xiao, C., Sakkiah, S., Guo, W., Gong, P., Zhang, C. *et al.* (2019) Similarities and differences between variants called with human reference genome HG19 or HG38. *BMC Bioinformatics*, **20**, 101.
4. Auton, A., Abecasis, G.R., Altshuler, D.M., Durbin, R.M., Abecasis, G.R., Bentley, D.R., Chakravarti, A., Clark, A.G., Donnelly, P., Eichler, E.E. *et al.* (2015) A global reference for human genetic variation. *Nature*, **526**, 68-74.
5. Ward, L.D. and Kellis, M. (2012) Interpreting noncoding genetic variation in complex traits and human disease. *Nature biotechnology*, **30**, 1095-1106.

6. Zhu, C., Miller, M., Zeng, Z., Wang, Y., Mahlich, Y., Aptekmann, A. and Bromberg, Y. (2020) Computational Approaches for Unraveling the Effects of Variation in the Human Genome and Microbiome. *Annual Review of Biomedical Data Science*, **3**.
7. Shen, H., Li, J., Zhang, J., Xu, C., Jiang, Y., Wu, Z., Zhao, F., Liao, L., Chen, J., Lin, Y. *et al.* (2013) Comprehensive Characterization of Human Genome Variation by High Coverage Whole-Genome Sequencing of Forty Four Caucasians. **8**, e59494.
8. Sauna, Z.E. and Kimchi-Sarfaty, C. (2011) Understanding the contribution of synonymous mutations to human disease. *Nature reviews. Genetics*, **12**, 683.
9. Stergachis, A.B., Haugen, E., Shafer, A., Fu, W., Vernot, B., Reynolds, A., Raubitschek, A., Ziegler, S., LeProust, E.M. and Akey, J.M. (2013) Exonic transcription factor binding directs codon choice and affects protein evolution. *Science*, **342**, 1367-1372.
10. Pagani, F., Raponi, M. and Baralle, F.E. (2005) Synonymous mutations in CFTR exon 12 affect splicing and are not neutral in evolution. *Proceedings of the National Academy of Sciences*, **102**, 6368-6372.
11. Chamary, J.V., Parmley, J.L. and Hurst, L.D. (2006) Hearing silence: non-neutral evolution at synonymous sites in mammals. *Nature Reviews Genetics*, **7**, 98-108.
12. Meyer, I.M. (2005) Statistical evidence for conserved, local secondary structure in the coding regions of eukaryotic mRNAs and pre-mRNAs. **33**, 6338-6348.
13. Duan, J., Shi, J., Ge, X., Dölken, L., Moy, W., He, D., Shi, S., Sanders, A.R., Ross, J. and Gejman, P.V. (2013) Genome-wide survey of interindividual differences of RNA stability in human lymphoblastoid cell lines. *Scientific reports*, **3**, 1318.
14. Shah, P., Ding, Y., Niemczyk, M., Kudla, G. and Joshua. (2013) Rate-Limiting Steps in Yeast Protein Translation. *Cell*, **153**, 1589-1601.
15. Pechmann, S. and Frydman, J. (2013) Evolutionary conservation of codon optimality reveals hidden signatures of cotranslational folding. *Nature structural & molecular biology*, **20**, 237.
16. Stoletzki, N. and Eyre-Walker, A. (2006) Synonymous codon usage in Escherichia coli: selection for translational accuracy. *Molecular biology and evolution*, **24**, 374-381.
17. Zeng, Z. and Bromberg, Y. (2019) Predicting Functional Effects of Synonymous Variants: A Systematic Review and Perspectives. *Frontiers in genetics*, **10**.
18. Buske, O.J., Manickaraj, A., Mital, S., Ray, P.N. and Brudno, M. (2013) Identification of deleterious synonymous variants in human genomes. *Bioinformatics*, **29**, 1843-1850.
19. Zhang, X., Li, M., Lin, H., Rao, X., Feng, W., Yang, Y., Mort, M., Cooper, D.N., Wang, Y. and Wang, Y. (2017) regSNPs-splicing: a tool for prioritizing synonymous single-nucleotide substitution. *Human genetics*, **136**, 1279-1289.
20. Livingstone, M., Folkman, L., Yang, Y., Zhang, P., Mort, M., Cooper, D.N., Liu, Y., Stantic, B. and Zhou, Y. (2017) Investigating DNA-, RNA-, and protein-based features as a means to discriminate pathogenic synonymous variants. *Human mutation*, **38**, 1336-1347.
21. Gelfman, S., Wang, Q., McSweeney, K.M., Ren, Z., La Carpia, F., Halvorsen, M., Schoch, K., Ratzon, F., Heinzen, E.L. and Boland, M.J. (2017) Annotating pathogenic non-coding variants in genic regions. *Nature communications*, **8**, 236.

22. Shi, F., Yao, Y., Bin, Y., Zheng, C.-H. and Xia, J. (2019) Computational identification of deleterious synonymous variants in human genomes using a feature-based approach. *BMC medical genomics*, **12**, 12.
23. Kircher, M., Witten, D.M., Jain, P., O'roak, B.J., Cooper, G.M. and Shendure, J. (2014) A general framework for estimating the relative pathogenicity of human genetic variants. *Nature genetics*, **46**, 310.
24. Rentzsch, P., Witten, D., Cooper, G.M., Shendure, J. and Kircher, M. (2019) CADD: predicting the deleteriousness of variants throughout the human genome. *Nucleic acids research*, **47**, D886-D894.
25. Quang, D., Chen, Y. and Xie, X. (2014) DANN: a deep learning approach for annotating the pathogenicity of genetic variants. *Bioinformatics*, **31**, 761-763.
26. Shihab, H.A., Rogers, M.F., Gough, J., Mort, M., Cooper, D.N., Day, I.N., Gaunt, T.R. and Campbell, C. (2015) An integrative approach to predicting the functional effects of non-coding and coding sequence variation. *Bioinformatics*, **31**, 1536-1543.
27. Schwarz, J.M., Cooper, D.N., Schuelke, M. and Seelow, D. (2014) MutationTaster2: mutation prediction for the deep-sequencing age. *Nature methods*, **11**, 361.
28. Stenson, P.D., Mort, M., Ball, E.V., Evans, K., Hayden, M., Heywood, S., Hussain, M., Phillips, A.D. and Cooper, D.N. (2017) The Human Gene Mutation Database: towards a comprehensive repository of inherited mutation data for medical research, genetic diagnosis and next-generation sequencing studies. *Human genetics*, **136**, 665-677.
29. Landrum, M.J., Lee, J.M., Riley, G.R., Jang, W., Rubinstein, W.S., Church, D.M. and Maglott, D.R. (2014) ClinVar: public archive of relationships among sequence variation and human phenotype. *Nucleic Acids Research*, **42**, D980-D985.
30. Bromberg, Y., Kahn, P.C. and Rost, B. (2013) Neutral and weakly nonneutral sequence variants may define individuality. **110**, 14255-14260.
31. Pejaver, V., Babbi, G., Casadio, R., Folkman, L., Katsonis, P., Kundu, K., Lichtarge, O., Martelli, P.L., Miller, M. and Moult, J. (2019) Assessment of methods for predicting the effects of PTEN and TPMT protein variants. *Human mutation*, **40**, 1495-1506.
32. Liu, B., Lee, W.S., Yu, P.S. and Li, X. (2002), *ICML*. Citeseer, Vol. 2, pp. 387-394.
33. Liu, B., Dai, Y., Li, X., Lee, W.S. and Yu, P.S. (2003), *Third IEEE International Conference on Data Mining*. IEEE, pp. 179-186.
34. Fusilier, D.H., Montes-y-Gómez, M., Rosso, P. and Cabrera, R.G. (2015) Detecting positive and negative deceptive opinions using PU-learning. *Information processing & management*, **51**, 433-443.
35. Mahlich, Y., Miller, M., Zeng, Z. and Bromberg, Y. (2021) Low diversity of human variation despite mostly mild functional impact of de novo variation. *Frontiers in Molecular Biosciences*, **8**, 74.
36. Kinsella, R.J., Kahari, A., Haider, S., Zamora, J., Proctor, G., Spudich, G., Almeida-King, J., Staines, D., Derwent, P., Kerhornou, A. *et al.* (2011) Ensembl BioMarts: a hub for data retrieval across taxonomic space. **2011**, bar030-bar030.

37. Church, D.M., Schneider, V.A., Graves, T., Auger, K., Cunningham, F., Bouk, N., Chen, H.-C., Agarwala, R., McLaren, W.M., Ritchie, G.R.S. *et al.* (2011) Modernizing Reference Genome Assemblies. **9**, e1001091.
38. Wang, K., Li, M. and Hakonarson, H. (2010) ANNOVAR: functional annotation of genetic variants from high-throughput sequencing data. *Nucleic Acids Research*, **38**, e164-e164.
39. Karczewski, K.J., Francioli, L.C., Tiao, G., Cummings, B.B., Alföldi, J., Wang, Q., Collins, R.L., Laricchia, K.M., Ganna, A., Birnbaum, D.P. *et al.* (2019) Variation across 141,456 human exomes and genomes reveals the spectrum of loss-of-function intolerance across human protein-coding genes. *bioRxiv*, 531210.
40. Lonsdale, J., Thomas, J., Salvatore, M., Phillips, R., Lo, E., Shad, S., Hasz, R., Walters, G., Garcia, F. and Young, N. (2013) The genotype-tissue expression (GTEx) project. *Nature genetics*, **45**, 580.
41. Sharp, P.M. and Li, W.-H. (1987) The codon adaptation index-a measure of directional synonymous codon usage bias, and its potential applications. *Nucleic acids research*, **15**, 1281-1295.
42. Ikemura, T. (1981) Correlation between the abundance of Escherichia coli transfer RNAs and the occurrence of the respective codons in its protein genes: a proposal for a synonymous codon choice that is optimal for the E. coli translational system. *Journal of molecular biology*, **151**, 389-409.
43. Karlin, S. and Mrázek, J. (1996) What drives codon choices in human genes? *Journal of molecular biology*, **262**, 459-472.
44. Freire-Picos, M.A., Gonzalez-Siso, M.I., Rodríguez-Belmonte, E., Rodriguez-Torres, A.M., Ramil, E. and Cerdan, M.E. (1994) Codon usage in Kluyveromyces lactis and in yeast cytochrome c-encoding genes. *Gene*, **139**, 43-49.
45. Wan, X., Xu, D. and Zhou, J. (2003) A new informatics method for measuring synonymous codon usage bias. *Intelligent engineering systems through artificial neural networks Volume*, **13**.
46. Dos Reis, M., Wernisch, L. and Savva, R. (2003) Unexpected correlations between gene expression and codon usage bias from microarray data for the whole Escherichia coli K-12 genome. *Nucleic acids research*, **31**, 6976-6985.
47. Team, R.C. (2013) R: A language and environment for statistical computing.
48. Supek, F. and Vlahoviček, K. (2005) Comparison of codon usage measures and their applicability in prediction of microbial gene expressivity. *BMC bioinformatics*, **6**, 182.
49. Cannarozzi, G., Schraudolph, N.N., Faty, M., Von Rohr, P., Friberg, M.T., Roth, A.C., Gonnet, P., Gonnet, G. and Barral, Y. (2010) A Role for Codon Order in Translation Dynamics. *Cell*, **141**, 355-367.
50. Yevshin, I., Sharipov, R., Valeev, T., Kel, A. and Kolpakov, F. (2016) GTRD: a database of transcription factor binding sites identified by ChIP-seq experiments. *Nucleic acids research*, gkw951.
51. Zhao, H., Sun, Z., Wang, J., Huang, H., Kocher, J.-P. and Wang, L. (2013) CrossMap: a versatile tool for coordinate conversion between genome assemblies. *Bioinformatics*, **30**, 1006-1007.
52. Giudice, G., Sánchez-Cabo, F., Torroja, C. and Lara-Pezzi, E. (2016) ATtRACT—a database of RNA-binding proteins and associated motifs. *Database*, **2016**.

53. Cáceres, E.F. and Hurst, L.D. (2013) The evolution, impact and properties of exonic splice enhancers. *Genome biology*, **14**, R143.
54. Yachdav, G., Kloppmann, E., Kajan, L., Hecht, M., Goldberg, T., Hamp, T., Hönigschmid, P., Schafferhans, A., Roos, M. and Bernhofer, M. (2014) PredictProtein—an open resource for online prediction of protein structural and functional features. *Nucleic acids research*, **42**, W337-W343.
55. Rost, B. (1996), *Methods in enzymology*. Elsevier, Vol. 266, pp. 525-539.
56. Schlessinger, A., Punta, M., Yachdav, G., Kajan, L. and Rost, B. (2009) Improved disorder prediction by combination of orthogonal approaches. *PloS one*, **4**, e4433.
57. Lorenz, R., Bernhart, S.H., Zu Siederdissen, C.H., Tafer, H., Flamm, C., Stadler, P.F. and Hofacker, I.L. (2011) ViennaRNA Package 2.0. *Algorithms for Molecular Biology*, **6**, 26.
58. Sabarinathan, R., Tafer, H., Seemann, S.E., Hofacker, I.L., Stadler, P.F. and Gorodkin, J. (2013) RNA snp: efficient detection of local RNA secondary structure changes induced by SNP s. *Human mutation*, **34**, 546-556.
59. LeCun, Y., Bengio, Y. and Hinton, G. (2015) Deep learning. *nature*, **521**, 436-444.
60. Chen, T. and Guestrin, C. (2016), *Proceedings of the 22nd acm sigkdd international conference on knowledge discovery and data mining*. ACM, pp. 785-794.
61. Chollet, F. (2015) Keras: Deep learning library for theano and tensorflow. *URL: https://keras. io/k*, **7**, T1.
62. Pedregosa, F., Varoquaux, G., Gramfort, A., Michel, V., Thirion, B., Grisel, O., Blondel, M., Prettenhofer, P., Weiss, R. and Dubourg, V. (2011) Scikit-learn: Machine learning in Python. *Journal of machine learning research*, **12**, 2825-2830.
63. Ionita-Laza, I., McCallum, K., Xu, B. and Buxbaum, J.D. (2016) A spectral approach integrating functional genomic annotations for coding and noncoding variants. *Nature genetics*, **48**, 214.
64. Landrum, M.J. and Kattman, B.L. (2018) ClinVar at five years: Delivering on the promise. *Human Mutation*, **39**, 1623-1630.
65. Davydov, E.V., Goode, D.L., Sirota, M., Cooper, G.M., Sidow, A. and Batzoglou, S. (2010) Identifying a high fraction of the human genome to be under selective constraint using GERP++. *PLoS computational biology*, **6**, e1001025.
66. Kumar, S., Stecher, G., Suleski, M. and Hedges, S.B. (2017) TimeTree: a resource for timelines, timetrees, and divergence times. *Molecular biology and evolution*, **34**, 1812-1819.
67. Zerbino, D.R., Achuthan, P., Akanni, W., Amode, M.R., Barrell, D., Bhai, J., Billis, K., Cummins, C., Gall, A. and Girón, C.G. (2017) Ensembl 2018. *Nucleic acids research*, **46**, D754-D761.
68. Löytynoja, A. and Goldman, N. (2005) An algorithm for progressive multiple alignment of sequences with insertions. *Proceedings of the National Academy of Sciences*, **102**, 10557-10562.
69. Cheung, R., Insigne, K.D., Yao, D., Burghard, C.P., Wang, J., Hsiao, Y.-H.E., Jones, E.M., Goodman, D.B., Xiao, X. and Kosuri, S. (2019) A multiplexed assay for exon recognition reveals that an unappreciated fraction of rare genetic variants cause large-effect splicing disruptions. *Molecular cell*, **73**, 183-194. e188.

70. Havrilla, J.M., Pedersen, B.S., Layer, R.M. and Quinlan, A.R. (2019) A map of constrained coding regions in the human genome. *Nature genetics*, **51**, 88-95.
71. Fakhro, K.A., Staudt, M.R., Ramstetter, M.D., Robay, A., Malek, J.A., Badii, R., Al-Marri, A.A.-N., Abi Khalil, C., Al-Shakaki, A. and Chidiac, O. (2016) The Qatar genome: a population-specific tool for precision medicine in the Middle East. *Human genome variation*, **3**, 1-7.
72. Leinonen, R., Sugawara, H., Shumway, M. and Collaboration, I.N.S.D. (2010) The sequence read archive. *Nucleic acids research*, **39**, D19-D21.
73. Dohm, J.C., Lottaz, C., Borodina, T. and Himmelbauer, H. (2008) Substantial biases in ultra-short read data sets from high-throughput DNA sequencing. *Nucleic acids research*, **36**, e105.
74. Rieber, N., Zapatka, M., Lasitschka, B., Jones, D., Northcott, P., Hutter, B., Jäger, N., Kool, M., Taylor, M. and Lichter, P. (2013) Coverage bias and sensitivity of variant calling for four whole-genome sequencing technologies. *PloS one*, **8**, e66621.
75. Forsdyke, D.R. (2001) Functional constraint and molecular evolution. *e LS*.
76. Alazami, A.M., Awad, S.M., Coskun, S., Al-Hassan, S., Hijazi, H., Abdulwahab, F.M., Poizat, C. and Alkuraya, F.S. (2015) TLE6 mutation causes the earliest known human embryonic lethality. *Genome biology*, **16**, 1-8.
77. Shamseldin, H.E., Tulbah, M., Kurdi, W., Nemer, M., Alsahan, N., Al Mardawi, E., Khalifa, O., Hashem, A., Kurdi, A. and Babay, Z. (2015) Identification of embryonic lethal genes in humans by autozygosity mapping and exome sequencing in consanguineous families. *Genome biology*, **16**, 116.
78. Hughes, A.L. (2008) Near-neutrality: the leading edge of the neutral theory of molecular evolution. *Annals of the New York Academy of Sciences*, **1133**, 162.
79. Eyre-Walker, A. and Keightley, P.D. (2007) The distribution of fitness effects of new mutations. *Nature Reviews Genetics*, **8**, 610-618.
80. Wall, J.D., Tang, L.F., Zerbe, B., Kvale, M.N., Kwok, P.-Y., Schaefer, C. and Risch, N. (2014) Estimating genotype error rates from high-coverage next-generation sequence data. *Genome research*, **24**, 1734-1739.
81. Lek, M., Karczewski, K.J., Minikel, E.V., Samocha, K.E., Banks, E., Fennell, T., O'Donnell-Luria, A.H., Ware, J.S., Hill, A.J., Cummings, B.B. *et al.* (2016) Analysis of protein-coding genetic variation in 60,706 humans. *Nature*, **536**, 285-291.
82. Bloom, J.S., Boocock, J., Treusch, S., Sadhu, M.J., Day, L., Oates-Barker, H. and Kruglyak, L. (2019) Rare variants contribute disproportionately to quantitative trait variation in yeast. *Elife*, **8**, e49212.
83. Purcell, S.M., Moran, J.L., Fromer, M., Ruderfer, D., Solovieff, N., Roussos, P., O'dushlaine, C., Chambert, K., Bergen, S.E. and Kähler, A. (2014) A polygenic burden of rare disruptive mutations in schizophrenia. *Nature*, **506**, 185-190.
84. Teng, S., Michonova-Alexova, E. and Alexov, E. (2008) Approaches and resources for prediction of the effects of non-synonymous single nucleotide polymorphism on protein function and interactions. *Current pharmaceutical biotechnology*, **9**, 123-133.
85. Genovese, G., Fromer, M., Stahl, E.A., Ruderfer, D.M., Chambert, K., Landén, M., Moran, J.L., Purcell, S.M., Sklar, P. and Sullivan, P.F. (2016) Increased burden of

ultra-rare protein-altering variants among 4,877 individuals with schizophrenia. *Nature neuroscience*, **19**, 1433-1441.

86. Bobbili, D.R., Banda, P., Krüger, R. and May, P. (2020) Excess of singleton loss-of-function variants in Parkinson's disease contributes to genetic risk. *Journal of Medical Genetics*.

87. Zhang, D., Cheng, L., Qian, Y., Alliey-Rodriguez, N., Kelsoe, J.R., Greenwood, T., Nievergelt, C., Barrett, T.B., McKinney, R. and Schork, N. (2009) Singleton deletions throughout the genome increase risk of bipolar disorder. *Molecular psychiatry*, **14**, 376-380.

88. Cooper, G.M. and Shendure, J. (2011) Needles in stacks of needles: finding disease-causal variants in a wealth of genomic data. *Nature Reviews Genetics*, **12**, 628-640.

89. Eilbeck, K., Quinlan, A. and Yandell, M. (2017) Settling the score: variant prioritization and Mendelian disease. *Nature Reviews Genetics*, **18**, 599-612.

90. MacArthur, D., Manolio, T., Dimmock, D., Rehm, H., Shendure, J., Abecasis, G., Adams, D., Altman, R., Antonarakis, S. and Ashley, E. (2014) Guidelines for investigating causality of sequence variants in human disease. *Nature*, **508**, 469-476.

91. Torkamani, A., Wineinger, N.E. and Topol, E.J. (2018) The personal and clinical utility of polygenic risk scores. *Nature Reviews Genetics*, **19**, 581-590.

92. Khera, A.V., Chaffin, M., Aragam, K.G., Haas, M.E., Roselli, C., Choi, S.H., Natarajan, P., Lander, E.S., Lubitz, S.A. and Ellinor, P.T. (2018) Genome-wide polygenic scores for common diseases identify individuals with risk equivalent to monogenic mutations. *Nature genetics*, **50**, 1219-1224.

93. Wang, Y., Miller, M., Astrakhan, Y., Petersen, B.-S., Schreiber, S., Franke, A. and Bromberg, Y. (2019) Identifying Crohn's disease signal from variome analysis. *Genome medicine*, **11**, 1-15.

94. Raimondi, D., Simm, J., Arany, A., Fariselli, P., Cleynen, I. and Moreau, Y. (2020) An interpretable low-complexity machine learning framework for robust exome-based in-silico diagnosis of Crohn's disease patients. *NAR Genomics and Bioinformatics*, **2**, lqaa011.

95. Capra, J.A., Stolzer, M., Durand, D. and Pollard, K.S. (2013) How old is my gene? *Trends in Genetics*, **29**, 659-668.

96. Briscoe, A.D., Gaur, C. and Kumar, S. (2004) The spectrum of human rhodopsin disease mutations through the lens of interspecific variation. *Gene*, **332**, 107-118.

97. Waterston, R.H. and Pachter, L. (2002) Initial sequencing and comparative analysis of the mouse genome. *Nature*, **420**, 520-562.

98. Kondrashov, A.S., Sunyaev, S. and Kondrashov, F.A. (2002) Dobzhansky–Muller incompatibilities in protein evolution. *Proceedings of the National Academy of Sciences*, **99**, 14878-14883.

99. Subramanian, S. and Kumar, S. (2006) Evolutionary anatomies of positions and types of disease-associated and neutral amino acid mutations in the human genome. *BMC genomics*, **7**, 306.

100. Li, W., Manktelow, E., von Kirchbach, J.C., Gog, J.R., Desselberger, U. and Lever, A.M. (2010) Genomic analysis of codon, sequence and structural conservation with selective biochemical-structure mapping reveals highly conserved and

dynamic structures in rotavirus RNAs with potential cis-acting functions. *Nucleic acids research*, **38**, 7718-7735.

101. Wang, G.-S. and Cooper, T.A. (2007) Splicing in disease: disruption of the splicing code and the decoding machinery. *Nature Reviews Genetics*, **8**, 749-761.
102. Supek, F., Miñana, B., Valcárcel, J., Gabaldón, T. and Lehner, B. (2014) Synonymous mutations frequently act as driver mutations in human cancers. *Cell*, **156**, 1324-1335.
103. Weile, J. and Roth, F.P. (2018) Multiplexed assays of variant effects contribute to a growing genotype–phenotype atlas. *Human genetics*, **137**, 665-678.
104. Richards, S., Aziz, N., Bale, S., Bick, D., Das, S., Gastier-Foster, J., Grody, W.W., Hegde, M., Lyon, E. and Spector, E. (2015) Standards and guidelines for the interpretation of sequence variants: a joint consensus recommendation of the American College of Medical Genetics and Genomics and the Association for Molecular Pathology. *Genetics in medicine*, **17**, 405-423.
105. Pertea, M., Lin, X. and Salzberg, S.L. (2001) GeneSplicer: a new computational method for splice site prediction. *Nucleic acids research*, **29**, 1185-1190.
106. Reese, M.G., Eeckman, F.H., Kulp, D. and Haussler, D. (1997) Improved splice site detection in Genie. *Journal of computational biology*, **4**, 311-323.
107. Comeron, J.M. and Kreitman, M. (1998) The correlation between synonymous and nonsynonymous substitutions in Drosophila: mutation, selection or relaxed constraints? *Genetics*, **150**, 767-775.
108. Wyckoff, G.J., Malcom, C.M., Vallender, E.J. and Lahn, B.T. (2005) A highly unexpected strong correlation between fixation probability of nonsynonymous mutations and mutation rate. *Trends in Genetics*, **21**, 381-385.
109. Li, J., Zhang, Z., Vang, S., Yu, J., Wong, G.K.-S. and Wang, J. (2009) Correlation between Ka/Ks and Ks is related to substitution model and evolutionary lineage. *Journal of molecular evolution*, **68**, 414-423.
110. Hurst, L.D. and Pál, C. (2001) Evidence for purifying selection acting on silent sites in BRCA1. *TRENDS in Genetics*, **17**, 62-65.
111. Orban, T.I. and Olah, E. (2001) Purifying selection on silent sites–a constraint from splicing regulation? *TRENDS in Genetics*, **17**, 252-253.
112. Parmley, J.L. and Hurst, L.D. (2007) How Common Are Intragene Windows with K A> K S Owing to Purifying Selection on Synonymous Mutations? *Journal of molecular evolution*, **64**, 646-655.
113. McVean, G.A. and Vieira, J. (2001) Inferring parameters of mutation, selection and demography from patterns of synonymous site evolution in Drosophila. *Genetics*, **157**, 245-257.
114. Nielsen, R., Bauer DuMont, V.L., Hubisz, M.J. and Aquadro, C.F. (2007) Maximum likelihood estimation of ancestral codon usage bias parameters in Drosophila. *Molecular Biology and Evolution*, **24**, 228-235.
115. Zhou, T., Gu, W. and Wilke, C.O. (2010) Detecting positive and purifying selection at synonymous sites in yeast and worm. *Molecular biology and evolution*, **27**, 1912-1922.
116. Lawrie, D.S., Messer, P.W., Hershberg, R. and Petrov, D.A. (2013) Strong purifying selection at synonymous sites in D. melanogaster. *PLoS Genet*, **9**, e1003527.

117. Lu, J. and Wu, C.-I. (2005) Weak selection revealed by the whole-genome comparison of the X chromosome and autosomes of human and chimpanzee. *Proceedings of the National Academy of Sciences*, **102**, 4063-4067.
118. Hellmann, I., Zöllner, S., Enard, W., Ebersberger, I., Nickel, B. and Pääbo, S. (2003) Selection on human genes as revealed by comparisons to chimpanzee cDNA. *Genome research*, **13**, 831-837.
119. Martin, A.R., Kanai, M., Kamatani, Y., Okada, Y., Neale, B.M. and Daly, M.J. (2019) Clinical use of current polygenic risk scores may exacerbate health disparities. *Nature genetics*, **51**, 584-591.
120. Karczewski, K.J., Francioli, L.C., Tiao, G., Cummings, B.B., Alföldi, J., Wang, Q., Collins, R.L., Laricchia, K.M., Ganna, A. and Birnbaum, D.P. (2020) The mutational constraint spectrum quantified from variation in 141,456 humans. *Nature*, **581**, 434-443.
121. Bromberg, Y., Kahn, P.C. and Rost, B. (2013) Neutral and weakly nonneutral sequence variants may define individuality. *Proceedings of the National Academy of Sciences*, **110**, 14255.